Published for SISSA by Springer

Received: *June 19, 2016*
Revised: *October 8, 2016*
Accepted: *February 8, 2017*
Published: *February 20, 2017*

Measurement of the transverse momentum spectra of weak vector bosons produced in proton-proton collisions at $\sqrt{s} = 8$ TeV

The CMS collaboration

E-mail: cms-publication-committee-chair@cern.ch

Abstract: The transverse momentum spectra of weak vector bosons are measured in the CMS experiment at the LHC. The measurement uses a sample of proton-proton collisions at $\sqrt{s} = 8$ TeV, collected during a special low-luminosity running that corresponds to an integrated luminosity of $18.4 \pm 0.5\,\mathrm{pb}^{-1}$. The production of W bosons is studied in both electron and muon decay modes, while the production of Z bosons is studied using only the dimuon decay channel. The ratios of W^- to W^+ and Z to W differential cross sections are also measured. The measured differential cross sections and ratios are compared with theoretical predictions up to next-to-next leading order in QCD.

Keywords: Hadron-Hadron scattering (experiments), QCD

ArXiv ePrint: 1606.05864

doi:10.1007/JHEP02(2017)096

JHEP02(2017)096

Contents

1 Introduction 1

2 The CMS detector 2

3 Data and simulated samples 3

4 Event selection 3

5 Measurement of the transverse momentum spectra 6
- 5.1 The W boson signal extraction 6
- 5.2 The Z boson signal extraction 7

6 Background estimation 8
- 6.1 The W boson analysis 8
- 6.2 The Z boson analysis 9

7 Systematic uncertainty 10

8 Results 11
- 8.1 The W and Z differential cross sections 12
- 8.2 Ratios of the cross sections 15

9 Summary 16

The CMS collaboration 25

JHEP02(2017)096

1 Introduction

Weak boson production processes, $q\bar{q} \to W + X$ and $q\bar{q} \to Z/\gamma^* + X$, play an important role at hadron colliders. Their clean leptonic final states allow for precise measurements with small experimental uncertainties that can be compared to theoretical predictions.

In proton-proton collisions, the W and Z bosons (denoted as V) are produced with zero transverse momentum p_T at leading order (LO). In a fixed-order perturbation theory, such a description shows a divergent behaviour of the p_T spectrum in the low-p_T region, which is sensitive to initial-state radiation and nonperturbative effects [1]. The high-p_T region is more sensitive to perturbative effects [2]; thus the experimental measurement of p_T^V constitutes a crucial test for both nonperturbative and perturbative quantum chromodynamics (QCD) calculations.

This paper reports a measurement of the W and Z boson p_T spectra and their ratios via electron and muon decay channels for the W and the muon decay channel for the Z boson within identical lepton fiducial volumes. The low-pileup data sample used in

this analysis was collected during low instantaneous luminosity proton-proton collisions at $\sqrt{s} = 8\,\text{TeV}$ [3]. This sample corresponds to an integrated luminosity of $18.4\,\text{pb}^{-1}$ and typically has only 4 collisions per bunch crossing (pileup) resulting in less background and improved resolution compared to ref. [4]. A finer binning at low Z boson p_{T} and a lower lepton p_{T} threshold of 20 GeV compared to the 25 GeV of ref. [4] also provide improvements over ref. [4].

The CDF and D0 Collaborations at the Fermilab Tevatron measured the W boson transverse momentum distribution in proton-antiproton collisions at $\sqrt{s} = 1.8\,\text{TeV}$ [5, 6] and the inclusive W and Z boson cross sections using the electron and muon decay channels at $\sqrt{s} = 1.96\,\text{TeV}$ [7]. The D0 Collaboration measured the differential cross sections of Z/γ^* production in the muon channel [8] and the p_{T} distribution of Z/γ^* production in the electron or muon channel in proton-antiproton collisions at $\sqrt{s} = 1.96\,\text{TeV}$ [9–11].

The high yield of W and Z boson events at the CERN LHC enables detailed studies of weak vector boson production mechanisms in different kinematic regions. The ATLAS and CMS Collaborations have performed several measurements of W and Z boson production via leptonic decays measured at both $\sqrt{s} = 7$ and 8 TeV. Measurements have been made of the inclusive W and Z boson cross sections in both electrons and muons [3, 12, 13] and of the Drell-Yan (DY) production differential cross section $\text{d}\sigma/\text{d}m$, where m is dilepton invariant mass [14, 15]. The cross sections as a function of p_{T} are measured for Z bosons [4, 16–18] and W bosons [19], but the latter has only been measured at $\sqrt{s} = 7\,\text{TeV}$. The LHCb Collaboration has measured the forward W and Z boson production cross sections and spectra for various kinematic variables at $\sqrt{s} = 7$ and 8 TeV using decays to lepton pairs [20–25]. All of the results are consistent with standard model (SM) expectations.

The total and differential DY production cross sections are currently calculated up to next-to-next-to-leading-order (NNLO) [2, 26] accuracy in perturbation theory, as implemented in the FEWZ (version 3.1) simulation code [27–29]. The theoretical treatment of soft-gluon emission is presently available to third order in the QCD coupling constant using resummation techniques as used in the RESBOS (P and CP versions) programs [30–32]. The measured cross sections can also be compared with predictions from an event generator like POWHEG (version 1.0) [33–36], which uses next-to-leading-order (NLO) QCD matrix elements. This package uses parton shower and hadronization processes implemented in PYTHIA (version 6.424) [37].

The paper is organized as follows. A brief description of the CMS detector is introduced in section 2. Event samples and Monte Carlo (MC) simulations are presented in section 3. We then describe the object reconstruction and event selection in section 4. These are followed by the background estimation and the measurement of W and Z boson p_{T} spectra in sections 6 and 5, respectively. The evaluation of the systematic uncertainties is described in section 7. We then present the results in section 8 and the summary in section 9.

2 The CMS detector

The central feature of the CMS apparatus is a superconducting solenoid of 6 m internal diameter that provides a magnetic field of 3.8 T. Within the solenoid volume are a silicon

JHEP02(2017)096

pixel and strip tracker, a lead tungstate crystal electromagnetic calorimeter (ECAL), and a brass and scintillator hadron calorimeter (HCAL), each composed of a barrel and two endcap sections. Extensive forward calorimetry complements the coverage provided by the barrel and endcap detectors. Muons are measured in gas-ionization detectors embedded in the steel flux-return yoke outside the solenoid. A more detailed description of the CMS detector, together with definitions of the coordinate system and the relevant kinematic variables such as pseudorapidity η, can be found in ref. [38].

3 Data and simulated samples

In this analysis, W boson candidates are reconstructed from their leptonic decays to electrons ($\mathrm{W} \to \mathrm{e}\nu_\mathrm{e}$) or muons ($\mathrm{W} \to \mu\nu_\mu$), while Z bosons are reconstructed only via their dimuon decays ($\mathrm{Z} \to \mu\mu$). The candidate events were collected by using dedicated single-lepton triggers for low instantaneous luminosity operation of the LHC that required the presence of an electron (muon) with $p_\mathrm{T} > 22\,(15)$ GeV and $|\eta| < 2.5\,(2.1)$.

The W and Z boson processes are generated with POWHEG at NLO accuracy using the parton distribution function (PDF) set CT10 [39]. The factorization and the renormalization scales in the POWHEG calculation are set to $(M_\mathrm{V}^2 + (p_\mathrm{T}^\mathrm{V})^2)^{1/2}$, where M_V and p_T^V refer to the mass and the transverse momentum, respectively, of the vector boson. For the background processes, parton showering and hadronization are implemented by using PYTHIA with the k_T-MLM prescription for the matrix element to parton showering matching, as described in ref. [40]. For the underlying event, the Z2* tune is used. The PYTHIA Z2* tune is derived from the Z1 tune [41], which uses the CTEQ5L PDF set, whereas Z2* adopts CTEQ6L [42].

The effect of QED final-state radiation (FSR) is implemented by using PYTHIA. The $\mathrm{Z} \to \tau\tau$ and diboson background event samples are generated with PYTHIA. Inclusive $\mathrm{t\bar{t}}$ and W + jets processes are generated with the MADGRAPH 5 (version 1.3.30) [43] LO matrix-element based generator package with $\mathrm{V}+n$-jets ($n = 0 \ldots 4$) predictions interfaced to PYTHIA using the CTEQ6L PDF set. The generated events are processed through the GEANT4-based [44] detector simulation, trigger emulation, and event reconstruction chain of the CMS experiment. Independently simulated pileup events with PYTHIA Z2* are superimposed on the generated event samples with a distribution that matches pileup events in data.

4 Event selection

The analysis uses the particle-flow (PF) algorithm [45, 46], which combines information from various detector subsystems to classify reconstructed objects or candidates according to particle type, thereby improving the precision of the particle energy and momentum measurements especially at low momenta.

The electron reconstruction combines electromagnetic clusters in ECAL and tracks reconstructed in the silicon tracker using the Gaussian Sum Filter algorithm (GSF) [47]. Electron candidates are selected by requiring a good agreement between track and cluster

JHEP02(2017)096

variables in position and energy, as well as no significant contribution in the HCAL [48]. Electrons from photon conversions are rejected by the vertex method described in ref. [49]. The magnitude of the transverse impact parameter is required to be <0.02 cm and the longitudinal distance from the interaction vertex is required to be <0.1 cm for electrons; this ensures that the electron candidate is consistent with a particle originating from the primary interaction vertex, which is the vertex with the highest p_{T}^2 sum of tracks associated to it.

The muon reconstruction starts from a candidate muon seed in the muon detectors followed by a global fit that uses information from the muon detectors and the silicon tracker [50]. The track associated with each muon candidate is required to have at least one hit in the pixel detector and at least five hits in different layers of the silicon tracker. The track is also required to have hits in at least two different muon detector planes. The magnitude of the transverse impact parameter is required to be <0.2 cm and the longitudinal distance from the interaction vertex is required to be <0.5 cm.

The missing transverse momentum vector $\vec{p}_{\mathrm{T}}^{\,\mathrm{miss}}$ in the event is defined as the projection of the negative vector sum of all the reconstructed particle momenta onto the plane perpendicular to the beam. Its magnitude is defined as missing transverse energy $E_{\mathrm{T}}^{\mathrm{miss}}$.

The analysis of the inclusive W boson production in the electron (muon) channel requires events with a single isolated electron (muon) with $p_{\mathrm{T}} > 25(20)$ GeV using the $E_{\mathrm{T}}^{\mathrm{miss}}$ distribution to evaluate the signal yield. Background events from QCD multijet processes are suppressed by requiring isolated leptons. For the W boson analysis, the isolation is based on the particle-flow information and is calculated by summing the p_{T} of charged hadrons and neutral particles in a cone with radius $\Delta R = \sqrt{(\Delta\eta)^2 + (\Delta\phi)^2} < 0.3\,(0.4)$ for electron (muon) events around the direction of the lepton at the interaction vertex

$$I_{\mathrm{PF}}^{\mathrm{e}} = \left(\sum p_{\mathrm{T}}^{\mathrm{charged}} + \max\left[0, \sum p_{\mathrm{T}}^{\mathrm{neutral}} + \sum p_{\mathrm{T}}^{\gamma} - \rho A_{\mathrm{eff}}\right]\right)/p_{\mathrm{T}}^{\mathrm{e}}, \tag{4.1a}$$

$$I_{\mathrm{PF}}^{\mu} = \left(\sum p_{\mathrm{T}}^{\mathrm{charged}} + \max\left[0, \sum p_{\mathrm{T}}^{\mathrm{neutral}} + \sum p_{\mathrm{T}}^{\gamma} - 0.5\sum p_{\mathrm{T}}^{\mathrm{PU}}\right]\right)/p_{\mathrm{T}}^{\mu}, \tag{4.1b}$$

where $\sum p_{\mathrm{T}}^{\mathrm{charged}}$ is the scalar p_{T} sum of charged hadrons originating from the primary vertex, $\sum p_{\mathrm{T}}^{\mathrm{PU}}$ is the energy deposited in the isolation cone by charged particles not associated with the primary vertex, and $\sum p_{\mathrm{T}}^{\mathrm{neutral}}$ and $\sum p_{\mathrm{T}}^{\gamma}$ are the scalar sums of the p_{T} for neutral hadrons and photons, respectively. A correction is included in the isolation variables to account for the neutral particles from pileup and underlying events. For electrons, the average transverse-momentum density ρ is calculated in each event by using the "jet area" A_{jet} [51], where ρ is defined as the median of the $p_{\mathrm{T}}^{\mathrm{jet}}/A_{\mathrm{jet}}$ distribution for all jets coming from pileup in the event, where $p_{\mathrm{T}}^{\mathrm{jet}}$ is the transverse momentum of a jet. This density is convolved with the effective area A_{eff} of the isolation cone, where the effective area A_{eff} is the geometric area of the isolation cone times an η-dependent correction factor that accounts for the residual dependence of the isolation on pileup. For muons, the correction is applied by subtracting $\sum p_{\mathrm{T}}^{\mathrm{PU}}$ multiplied by a factor 0.5. This factor corresponds approximately to the ratio of neutral to charged particle production in the hadronization process. The W boson events are selected if $I_{\mathrm{PF}}^{\mathrm{e}} < 0.15$ or $I_{\mathrm{PF}}^{\mu} < 0.12$.

JHEP02(2017)096

For the W boson analysis, events with a second electron with $p_{\mathrm{T}}^{\mathrm{e}} > 20\,\mathrm{GeV}$ or a second muon with $p_{\mathrm{T}}^{\mu} > 17\,\mathrm{GeV}$ that passes loose selection criteria are rejected as W boson events to reduce the background contributions from the Z/γ^* DY processes. The second electron selection uses a loose selection working point [48], which mainly relaxes the match of the energy and position between the GSF tracks and the associated clusters in the ECAL. For the second muon, the required number of hits in the pixel detector, the silicon tracker, and the muon detector are relaxed [50].

Several corrections are applied to the simulated events to account for the observed small discrepancies between data and simulation. A better description of the data is obtained by applying corrections to the lepton p_{T} and $E_{\mathrm{T}}^{\mathrm{miss}}$. There are two main sources of disagreement in the p_{T} description: the momentum scale and the modeling of the p_{T} resolution. The corrections for these effects are determined from a comparison of the $\mathrm{Z} \to \ell^+\ell^-$ mass spectrum between data and simulation [13]. The lepton momentum scale correction factor is found to be close to unity with an uncertainty of 0.2% (0.1%) for electrons (muons). An additional smearing of the lepton p_{T}- and η-dependent resolution in the range 0.4 to 0.9 (0.1 to 0.7) GeV for electrons (muons) is applied to reproduce the distribution of the dilepton invariant mass observed in data.

The vector boson recoil is defined as the vector sum of the transverse momenta of all the observed particles, excluding the leptons produced in the vector boson decay. The $E_{\mathrm{T}}^{\mathrm{miss}}$ spectra in the W boson signal simulation rely on the modeling of the W boson recoil and the simulation of the detector response. The correction factors for the W boson recoil simulation are estimated using a comparison of the Z boson recoil between data and simulation [13, 52]. The factors for the recoil scale (resolution) range from 0.88 to 0.98 (from 0.84 to 1.09) as a function of the boson p_{T} with an uncertainty of about 3 (5)%. They are applied to the simulated W boson recoil distributions.

The corrected $E_{\mathrm{T}}^{\mathrm{miss}}$ and corrected lepton momenta are used to calculate the transverse mass M_{T} of the W,

$$M_{\mathrm{T}} = \sqrt{2\, p_{\mathrm{T}}^{\ell}\, E_{\mathrm{T}}^{\mathrm{miss}} (1 - \cos \Delta\phi_{E_{\mathrm{T}}^{\mathrm{miss}},\ell})}, \tag{4.2}$$

where $\Delta\phi_{E_{\mathrm{T}}^{\mathrm{miss}},\ell}$ is the azimuthal angle between $\vec{p}_{\mathrm{T}}^{\mathrm{miss}}$ and lepton $\vec{p_{\mathrm{T}}}$. M_{T} is used for the signal yield extraction for the muon channel in the high-p_{T} region, as described in section 5.1.

A set of lepton efficiencies, namely the lepton reconstruction and identification, and trigger efficiencies, are estimated in simulation and then corrected for the differences between data and simulation. These corrections are evaluated by using a "tag-and-probe" method [53] and the total efficiency correction factor for the simulated samples ranges between 0.92 ± 0.03 (0.93 ± 0.05) and 1.03 ± 0.08 (1.04 ± 0.03) for electrons (muons).

For the inclusive Z boson events we require two isolated oppositely charged muons with $p_{\mathrm{T}} > 20\,\mathrm{GeV}$. A vertex fit is performed to ensure that the candidates originate from the same Z boson. The background due to cosmic ray muons passing through the detector and mimicking dimuon events is suppressed by requiring that the two muons are not back-to-back, i.e. the three-dimensional opening angle between the two muons should be smaller

JHEP02(2017)096

than $\pi - 0.02$ radians. Finally, the muon pair is required to have a reconstructed invariant mass in the range 60–120 GeV.

For the Z boson analysis, the dimuon invariant mass selection and a vertex fit enables the use of a simpler isolation variable based only on charged tracks. The track isolation variable I_{trk} is defined as the scalar sum of the track momenta of charged particles lying within a cone of radius $\Delta R = 0.3$ around the muon direction. The muons are isolated if $I_{\mathrm{trk}}/p_{\mathrm{T}}^{\mu} < 0.1$.

5 Measurement of the transverse momentum spectra

The transverse momentum of the vector boson $p_{\mathrm{T}}^{\mathrm{V}}$ is computed from the momentum sum of the decay leptons for the Z boson, or the lepton and $\vec{p}_{\mathrm{T}}^{\,\mathrm{miss}}$ for the W boson. The measurements are performed within the lepton fiducial volumes defined by $p_{\mathrm{T}} > 25\,(20)$ GeV, $|\eta| < 2.5\,(2.1)$ for the electron (muon) channel. The fiducial region for the boson differential cross section is defined by the p_{T} and η requirements on the leptons.

The transverse momentum spectra are analyzed as binned histograms, with bin widths varying from 7.5 (2.5) GeV for the W (Z) boson up to 350 GeV, in order to provide sufficient resolution to observe the shape of the distribution, limit the migration of events between neighbouring bins, and ensure a sufficient number of events in each bin. The cross section in the ith $p_{\mathrm{T}}^{\mathrm{V}}$ bin is defined as

$$\frac{\mathrm{d}\sigma_i}{\mathrm{d}p_{\mathrm{T},\,i}^{\mathrm{V}}} = \frac{N_i}{\Delta_i\,\epsilon_i \int L\mathrm{d}t}, \tag{5.1}$$

where N_i is the estimated number of signal events in the bin, Δ_i is the width of the bin, ϵ_i is the efficiency of the event selection in that bin, and $\int L\mathrm{d}t$ is the integrated luminosity.

The differential distributions are unfolded to the lepton level before QED final-state radiation (pre-FSR) within the same fiducial volume.

5.1 The W boson signal extraction

The W boson signal yield and the backgrounds for each $p_{\mathrm{T}}^{\mathrm{W}}$ bin are determined using an extended likelihood fit to the $E_{\mathrm{T}}^{\mathrm{miss}}$ distributions. The fits constrain the sum of signal plus background to the data within each bin. Figure 1 shows an example of the fit for the bin $17.5 < p_{\mathrm{T}}^{\mathrm{W}} < 24$ GeV. The signal and background shapes are determined separately for W^+ and W^- bosons to account for the difference in the kinematical configuration arising from the parity-violating nature of the weak interaction. The signal yield and background contaminations are estimated from the fit, which is performed simultaneously in the signal candidate sample and in the corresponding QCD control sample for each $p_{\mathrm{T}}^{\mathrm{W}}$ bin. The QCD multijet-enriched control samples are defined by inverting the selection on some identification variables for the electron channel, and by inverting the isolation requirement for the muon channel, while maintaining the rest of the signal selection criteria.

The W boson signal and electroweak (EW) background (explained in section 6) templates are produced by using simulated events including all corrections described in section 4. The EW contribution is constrained for the W signal yield by fixing the ratio of

JHEP02(2017)096

the theoretical cross section of the EW contribution to that of W boson production. The QCD shape of $E_{\mathrm{T}}^{\mathrm{miss}}$ distribution is parameterized by a modified Rayleigh function [3],

$$f(x) = x \exp\left(-\frac{x^2}{2(\sigma_0 + \sigma_1 x)^2}\right), \tag{5.2}$$

where σ_0 and σ_1 are free parameters of the fit. The fit uses $x = E_{\mathrm{T}}^{\mathrm{miss}}$ for $p_{\mathrm{T}}^{\mathrm{W}} > 17.5\,\mathrm{GeV}$ and $x = (E_{\mathrm{T}}^{\mathrm{miss}} - a)$ for $p_{\mathrm{T}}^{\mathrm{W}} < 17.5\,\mathrm{GeV}$, where a is a parameter of the fit needed to take into account the minimum $E_{\mathrm{T}}^{\mathrm{miss}}$ value at each $p_{\mathrm{T}}^{\mathrm{W}}$ bin due to trigger requirements on the p_{T}^{ℓ}. The parameter σ_0 in eq. (5.2) is, however, kept floating separately in signal and control regions.

In the muon channel, the QCD multijet contribution decreases noticeably with increasing $p_{\mathrm{T}}^{\mathrm{W}}$ because the probability of the background muon to pass the isolation criteria decreases. For $p_{\mathrm{T}}^{\mathrm{W}} > 70\,\mathrm{GeV}$ the M_{T} distributions, instead of $E_{\mathrm{T}}^{\mathrm{miss}}$, are fitted to maintain a good separation between the signal and the QCD background shape. The extracted signal and background yields are shown as a function of $p_{\mathrm{T}}^{\mathrm{W}}$ in figure 2 for electrons (upper) and muons (lower).

In order to obtain the differential cross section before FSR, the detector resolution and FSR effects need to be corrected. This is achieved by a two-step unfolding process using the singular value decomposition (SVD) method [54]. SVD uses two response matrices. The first matrix maps the intra-bin migration effects to the reconstructed $p_{\mathrm{T}}^{\mathrm{W}}$ from leptons after a possible FSR (post-FSR) effect, using the POWHEG simulated signal sample as the baseline, after applying lepton momentum resolution, efficiency, and recoil corrections. The second matrix maps the $p_{\mathrm{T}}^{\mathrm{W}}$ distribution taking into account the FSR effect of the lepton, i.e. from pre-FSR to post-FSR.

The event reconstruction efficiency is corrected bin-by-bin after unfolding for the detector resolution by using the simulated signal sample. An acceptance correction is applied to the pre-FSR distribution after FSR unfolding; about 5.1% (1.9%) of the events with a pre-FSR level electron (muon) generated within the fiducial region do not pass the post-FSR lepton requirements of the fiducial volume.

5.2 The Z boson signal extraction

The number of observed Z boson events is obtained by subtracting the estimated number of background events from the total number of detected events in each of the $p_{\mathrm{T}}^{\mathrm{Z}}$ bins. The transverse momentum distribution of the dimuon system for the reconstructed events is shown in figure 3 separately for the low- and high-$p_{\mathrm{T}}^{\mathrm{Z}}$ regions to show the level of agreement between data and simulation. The NLO QCD calculation in POWHEG underestimates the data by 27% in the $p_{\mathrm{T}}^{\mathrm{Z}}$ range below 2.5 GeV.

The measured $p_{\mathrm{T}}^{\mathrm{Z}}$ distributions are corrected for bin migration effects that arise from the detector resolution and FSR effects with a similar technique to the W boson analysis described in section 5.1 using a matrix-based unfolding procedure [55]. The final result is corrected by the bin width and is normalized by the measured total cross section σ within the fiducial region (section 5) in the range of the dimuon mass, $60 < m_{\mu\mu} < 120\,\mathrm{GeV}$.

JHEP02(2017)096

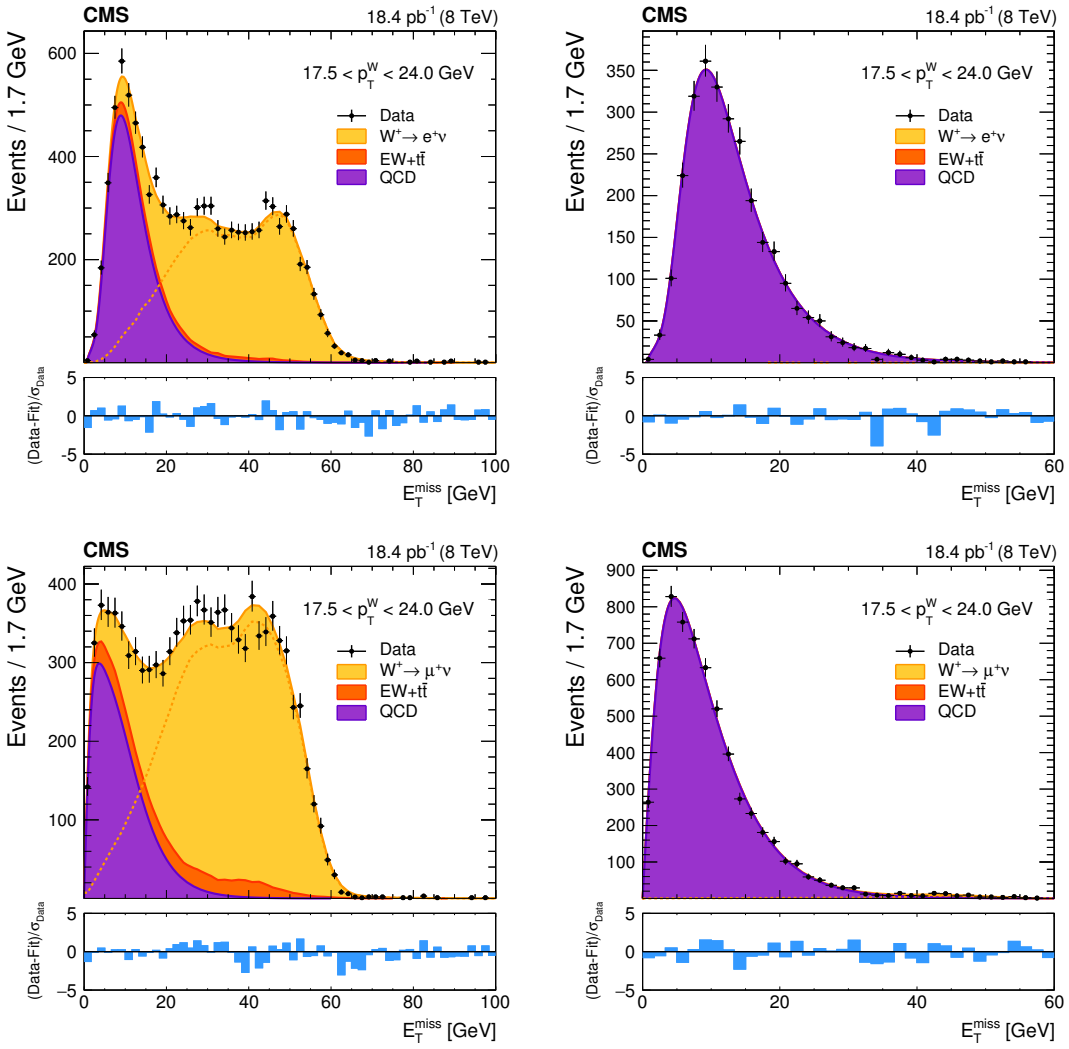

Figure 1. The $E_{\mathrm{T}}^{\mathrm{miss}}$ distributions for the selected $\mathrm{W}^+ \to \mathrm{e}^+\nu$ (upper) and $\mathrm{W}^+ \to \mu^+\nu$ (lower) candidates for $17.5 < p_{\mathrm{T}}^{\mathrm{W}} < 24\,\mathrm{GeV}$ (left) and the corresponding QCD multijet-enriched control sample (right). Solid lines represent the results of the fit. The dotted lines represent the signal shape after background subtraction. The bottom panels show the difference between data and fitted results divided by the statistical uncertainty in data, σ_{Data}.

6 Background estimation

6.1 The W boson analysis

QCD multijet events are the dominant source of background in the W boson analysis. The level of contamination is estimated from data as described in section 5.1. It is about 40% and 19% of the selected $\mathrm{W} \to \mathrm{e}\nu$ and $\mathrm{W} \to \mu\nu$ event yields, respectively.

The contributions of EW and $\mathrm{t\bar{t}}$ background sources are estimated by using simulated events. The DY processes with $\mathrm{Z}/\gamma^* \to \ell^+\ell^-$ contribute to the $\mathrm{W} \to \ell\nu$ background when one of the two leptons is not detected. These processes account for approximately 4.7% (5.0%) of the selected events in the electron (muon) channel. Events from $\mathrm{W} \to \tau\nu$ (where

JHEP02(2017)096

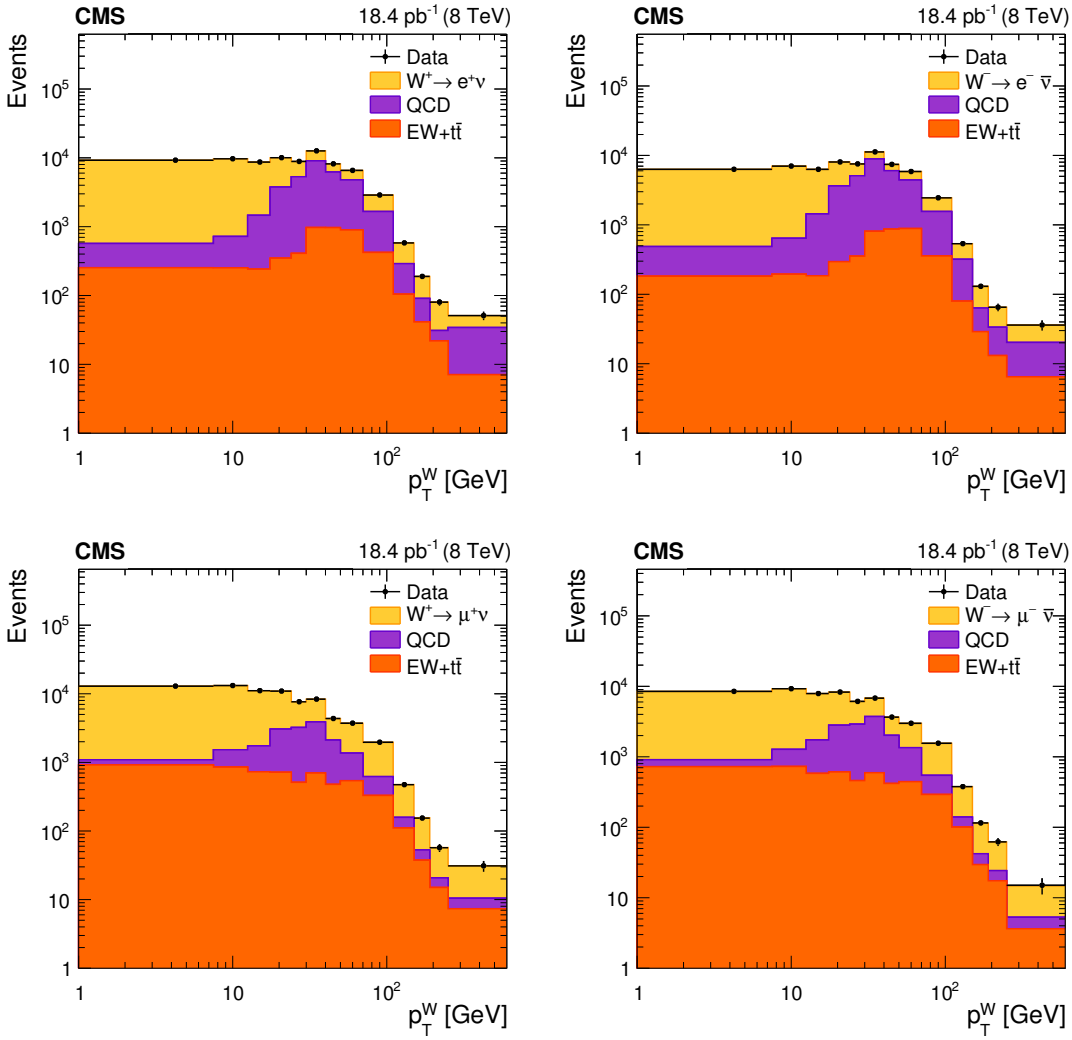

Figure 2. Signal and background yields after fitting the data for $W^+ \to e^+\nu$ (upper left), $W^- \to e^-\overline{\nu}$ (upper right), $W^+ \to \mu^+\nu$ (lower left), and $W^- \to \mu^-\overline{\nu}$ (lower right) as a function of the W boson p_T. The points are data yields with statistical uncertainties. The stacked histogram shows the signal and background components estimated from a fit to the E_T^{miss} or M_T distribution at each W boson p_T bin.

the τ decays leptonically) have, in general, a softer lepton than the signal events. They are strongly suppressed by using a high value of the minimum $p_T^{e,\mu}$ requirement for acceptance. The background contribution from $W \to \tau\nu$ is 1.7% (3.3%) of selected events in the electron (muon) channel. The background originating from $t\bar{t}$ production is estimated to be 0.35% (0.41%) of the selected events, while that from boson pair production (WW, WZ, and ZZ) is even smaller, about 0.03% of the selected events for both decay channels.

6.2 The Z boson analysis

The main sources of background in the dimuon analysis are $Z \to \tau\tau$, $t\bar{t}$, W+jets, and diboson (WW, WZ, and ZZ) production with the subsequent decay of W, Z, and τ to

JHEP02(2017)096

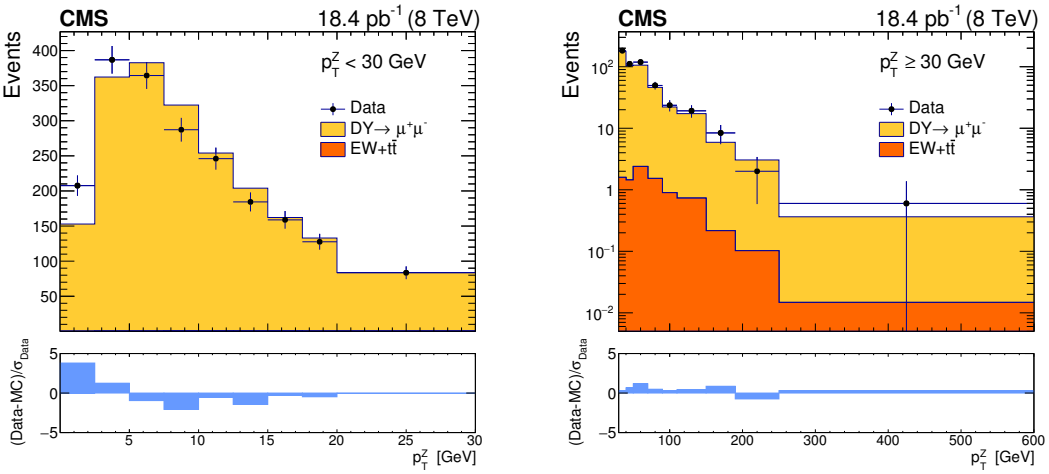

Figure 3. Data and simulated events for both DY processes and various backgrounds after event reconstruction. Left (right): events for low (high) $p_{\mathrm{T}}^{\mathrm{Z}}$, $p_{\mathrm{T}}^{\mathrm{Z}} < 30$ (≥ 30) GeV. The lower panels show the difference between the data and the simulation predictions divided by the statistical uncertainty in data, σ_{Data}.

muons. The simulation of these backgrounds is validated with data by measuring the p_{T} of the final state with an electron and a muon. The residual background contribution is due to QCD multijet hadronic processes that contain energetic muons, predominantly from the semileptonic decays of B hadrons. A control sample of events with a single muon that passes all the requirements of this analysis except the isolation criteria is selected to estimate the contribution of this source. This sample is subsequently used to estimate the probability for a muon to pass the isolation requirements as a function of the muon p_{T} and η. This probability is used to predict the number of background events with two isolated muons based on a sample of events with two nonisolated muons. This procedure, which is validated by using simulated events, predicts a negligible contribution from QCD multijet production over the full range of our $p_{\mathrm{T}}^{\mathrm{Z}}$ spectrum. After the full selection, the background contamination, which consists primarily of $\mathrm{Z} \to \tau\tau$ and $\mathrm{t\bar{t}}$ processes, with an uncertainty dominated by the statistical uncertainties in the background simulation is estimated to be less than 1% of the total event yield.

7 Systematic uncertainty

The leading sources of systematic uncertainties are mostly common to both the W and Z boson analyses. They include the determination of the correction factors for the lepton efficiency (reconstruction, isolation, and trigger), the electron or muon momentum resolution parameters, and the construction of the response matrices for unfolding the detector resolution and FSR effects. The simulated distributions are corrected for the efficiency differences between data and simulation using scale factors obtained from the tag-and-probe method. The variation of the measured scale factors due to different choices of signal and background models and the p_{T} and η binnings for the measured lepton are treated as sys-

JHEP02(2017)096

Channel	$\sigma\,\mathcal{B}$ [nb] (fiducial)
$\mathrm{Z} \to \mu^+\mu^-$	$0.44 \pm 0.01\,(\mathrm{stat}) \pm 0.01\,(\mathrm{syst}) \pm 0.01\,(\mathrm{lumi})$
$\mathrm{W} \to \mathrm{e}\nu$	$6.27 \pm 0.03\,(\mathrm{stat}) \pm 0.10\,(\mathrm{syst}) \pm 0.16\,(\mathrm{lumi})$
$\mathrm{W} \to \mu\nu$	$6.29 \pm 0.02\,(\mathrm{stat}) \pm 0.09\,(\mathrm{syst}) \pm 0.16\,(\mathrm{lumi})$

Table 1. The fiducial cross sections at pre-FSR level calculated as the sum of differential cross sections. The fiducial volumes are defined in section 5.

tematic uncertainties. The momentum resolution is estimated by comparing data and the simulated Z boson mass distribution. The uncertainties in the parameterization of the mass distribution are propagated in the resolution calculation. The uncertainty in the model-dependent FSR simulation is estimated by reweighting the simulated data samples. We are using event-dependent weights from a soft collinear approach [56] and higher-order corrections in $\alpha(p_{\mathrm{T}}^2)$ [57]. The difference in signal yields before and after reweighting is assigned as a systematic uncertainty. The systematic uncertainty in the luminosity measurement is completely canceled out since the results are presented as normalized distributions.

The uncertainty in the recoil corrections to $E_{\mathrm{T}}^{\mathrm{miss}}$ is taken into account for the W boson analysis. The systematic uncertainty associated with the shape of the $E_{\mathrm{T}}^{\mathrm{miss}}$ distribution from the QCD multijet process is estimated by introducing an additional term $\sigma_2 x^2$ into eq. (5.2), where σ_2 is another shape parameter to describe the tail of $E_{\mathrm{T}}^{\mathrm{miss}}$ at the second order, and repeating the fit procedure. A set of pseudo-experiments is generated by varying all parameters of the equation within their uncertainties. The bias in the measured values with the pseudo-experiments provides the systematic uncertainty in the parameterization of the shape. An additional uncertainty is assigned due to the simultaneous fit procedure by floating the tail parameter σ_1 in the extraction of the signal yields. These are used to estimate the shape dependence of the fits to the QCD multijet-enriched control samples.

The cross section for each of the EW backgrounds in the W boson analysis is varied around the central value within its uncertainty and the resulting fluctuation of signal yield extraction by the fit in each $p_{\mathrm{T}}^{\mathrm{W}}$ bin is assigned as a systematic uncertainty.

The unfolding procedure is sensitive to the statistical uncertainties in the construction of the response matrix. These uncertainties range from 0.1% to 1.0% depending on the channel and $p_{\mathrm{T}}^{\mathrm{V}}$ bin. The boson distributions are compared with those obtained by using an alternative response matrix derived from a different generator, MadGraph 5. The difference is taken as the unfolding bias.

The background for the dimuon final state is measured from simulation with correction factors derived from data, the corresponding uncertainty is estimated by varying its contribution. The uncertainty is about 0.4% level up to 40 GeV of dimuon p_{T}.

8 Results

The fiducial cross sections at pre-FSR level are calculated as the sum of contributions from all bins and listed in table 1.

JHEP02(2017)096

The low-pileup data is adjusted to the lepton fiducial volume at post-FSR level used in ref. [3]. The results are $0.40 \pm 0.01\,(\text{stat}) \pm 0.01\,(\text{syst}) \pm 0.01\,(\text{lumi})$ nb for the Z channel and $5.47 \pm 0.02\,(\text{stat}) \pm 0.06\,(\text{syst}) \pm 0.14\,(\text{lumi})$ nb for the mean value of W electron and muon channel results weighted by uncertainties. These are consistent with the supplemental material of ref. [3], where the fiducial inclusive Z boson cross section is $0.40 \pm 0.01\,(\text{stat}) \pm 0.01\,(\text{syst}) \pm 0.01\,(\text{lumi})$ nb and the W boson cross section is $5.42 \pm 0.02\,(\text{stat}) \pm 0.06\,(\text{syst}) \pm 0.14\,(\text{lumi})$ nb.

The differential cross sections $\mathrm{d}\sigma/\mathrm{d}p_{\mathrm{T}}^{\mathrm{V}}$, corrected for FSR, are normalized to the total fiducial cross section. Some uncertainties are canceled in the normalized cross sections, thus allowing for a more precise shape comparison. The uncertainties in the measurement of the lepton efficiencies are decreased by factors of 1.6 to 7.7 with respect to the cross section before the normalization. The uncertainties in the EW background cross sections affect both the numerator and the denominator, hence the corresponding uncertainty is decreased by a factor of 20. The other sources of uncertainty remain at a level similar to the differential cross section measurements before normalization.

The differential cross sections in the electron and muon channels, derived individually for W^+ and W^- bosons, are combined after taking into account the possible correlations. The systematic uncertainties due to FSR and EW background cross sections are added linearly under the assumption that these uncertainties are 100% correlated. All other charge-dependent uncertainties are assumed to be uncorrelated and are added in quadrature.

The data unfolded to the pre-FSR level are compared to various theoretical predictions: ResBos-P version (CP version) with scale (scale and PDF) variation for the W (Z) boson result, powheg with PDF uncertainty, and fewz with PDF and renormalization and factorization scale uncertainties. ResBos adopts the Collins-Soper-Sterman formalism with four parameters (C1, C2, C3, and C4) for the resummation of the multiple and collinear gluon emissions [58, 59], which yields a next-to-next-to-leading-order accuracy. It allows also for the use of a K factor grid to get an effective NNLO description. The scale parameters in C2 (μ_F) and C4 (for α_s and PDF) are set to $M_{\ell\ell}/2$ (where $M_{\ell\ell}$ is the invariant mass of the lepton pair) as the nominal value and different grid points are generated with scale variations $M_{\ell\ell}$ and $M_{\ell\ell}/4$ for the determination of the scale uncertainty. The nonperturbative function implemented in ResBos affects mostly the low-p_{T} region around 1–4 GeV and the intermediate-p_{T} region with small contribution.

8.1 The W and Z differential cross sections

The numerical results and all of the uncertainties for the normalized differential cross section are listed in tables 2 and 3 for the electron and muon channels of the W boson decay, respectively. The results for the $p_{\mathrm{T}}^{\mathrm{Z}}$ spectrum are summarized in table 4. After combining the effects discussed in section 7, the total systematic uncertainty in each bin is found to be smaller than the corresponding statistical uncertainty for the Z boson and at a similar level for the W boson except in the high-$p_{\mathrm{T}}^{\mathrm{W}}$ region.

The results are compared to three different theoretical predictions: ResBos, powheg, and fewz using CT10 [39] PDFs with uncertainties estimated by the method described in

JHEP02(2017)096

Bin (GeV)	Lept. recon.	Mom. res.	$E_{\mathrm{T}}^{\mathrm{miss}}$ res.	QCD bkgr.	QCD shape	EW	SVD unfld.	FSR	Unfld. bias	Total syst.	Stat.	$(1/\sigma)(\mathrm{d}\sigma/\mathrm{d}p_{\mathrm{T}})$ (GeV^{-1})
0–7.5	0.31	0.21	0.22	0.51	0.20	0.05	0.08	0.05	0.75	1.03	0.60	$(4.74 \pm 0.06) \times 10^{-2}$
7.5–12.5	0.26	0.09	0.10	0.64	0.26	0.04	0.08	0.05	1.43	1.62	0.74	$(4.12 \pm 0.07) \times 10^{-2}$
12.5–17.5	0.17	0.24	0.10	0.48	0.37	0.02	0.08	0.04	1.11	1.31	0.89	$(2.42 \pm 0.04) \times 10^{-2}$
17.5–24	0.16	0.30	0.27	0.66	0.43	0.04	0.09	0.00	0.36	0.98	0.95	$(1.49 \pm 0.02) \times 10^{-2}$
24–30	0.37	0.26	0.35	0.80	0.51	0.05	0.10	0.06	0.58	1.25	1.28	$(9.64 \pm 0.17) \times 10^{-3}$
30–40	0.62	0.23	0.34	1.27	0.40	0.09	0.12	0.12	0.29	1.56	1.28	$(6.07 \pm 0.12) \times 10^{-3}$
40–50	0.86	0.33	0.26	0.86	0.45	0.12	0.14	0.17	0.34	1.43	1.71	$(3.51 \pm 0.08) \times 10^{-3}$
50–70	1.09	0.46	0.17	1.74	0.58	0.16	0.16	0.20	0.47	2.26	1.75	$(1.78 \pm 0.05) \times 10^{-3}$
70–110	1.28	0.35	0.13	0.79	0.63	0.18	0.19	0.22	2.30	2.87	2.16	$(5.66 \pm 0.20) \times 10^{-4}$
110–150	1.44	0.51	0.14	1.37	0.62	0.20	0.22	0.25	2.31	3.18	4.46	$(1.45 \pm 0.08) \times 10^{-4}$
150–190	1.55	1.24	0.17	1.25	0.47	0.22	0.24	0.29	4.57	5.18	7.74	$(4.54 \pm 0.42) \times 10^{-5}$
190–250	1.62	1.04	0.20	1.19	0.62	0.23	0.26	0.29	2.96	3.81	11.14	$(1.50 \pm 0.18) \times 10^{-5}$
250–600	1.65	0.62	0.20	1.78	0.66	0.23	0.27	0.34	4.07	4.85	18.07	$(1.18 \pm 0.22) \times 10^{-6}$

Table 2. The W boson normalized differential cross sections for the electron channel in bins of $p_{\mathrm{T}}^{\mathrm{W}}$, $(1/\sigma)(\mathrm{d}\sigma/\mathrm{d}p_{\mathrm{T}})$ ($\mathrm{W} \to \mathrm{e}\nu$), and systematic uncertainties from various sources in units of %, where σ is the sum of the cross sections for the $p_{\mathrm{T}}^{\mathrm{W}}$ bins. $(1/\sigma)(\mathrm{d}\sigma/\mathrm{d}p_{\mathrm{T}})$ is shown with total uncertainty, i.e. the sum of statistical and systematic uncertainties in quadrature.

Bin (GeV)	Lept. recon.	Mom. res.	$E_{\mathrm{T}}^{\mathrm{miss}}$ res.	QCD bkgr.	QCD shape	EW	SVD unfld.	FSR	Unfld. bias	Total syst.	Stat.	$(1/\sigma)(\mathrm{d}\sigma/\mathrm{d}p_{\mathrm{T}})$ (GeV^{-1})
0–7.5	0.22	0.11	0.04	0.62	0.17	0.00	0.14	0.00	0.93	1.16	0.51	$(4.88 \pm 0.06) \times 10^{-2}$
7.5–12.5	0.11	0.06	0.02	0.95	0.26	0.02	0.12	0.00	1.72	1.99	0.65	$(4.16 \pm 0.09) \times 10^{-2}$
12.5–17.5	0.18	0.09	0.04	0.87	0.22	0.03	0.14	0.00	1.15	1.48	0.79	$(2.37 \pm 0.04) \times 10^{-2}$
17.5–24	0.32	0.20	0.06	0.94	0.27	0.04	0.17	0.00	0.30	1.11	0.85	$(1.43 \pm 0.02) \times 10^{-2}$
24–30	0.40	0.25	0.06	0.94	0.28	0.02	0.18	0.00	0.65	1.28	1.14	$(9.25 \pm 0.16) \times 10^{-3}$
30–40	0.38	0.24	0.06	1.52	0.26	0.03	0.19	0.01	0.27	1.64	1.14	$(5.91 \pm 0.12) \times 10^{-3}$
40–50	0.31	0.17	0.06	0.89	0.15	0.06	0.21	0.01	0.44	1.09	1.58	$(3.50 \pm 0.07) \times 10^{-3}$
50–70	0.29	0.14	0.07	1.47	0.31	0.10	0.26	0.01	0.78	1.74	1.57	$(1.77 \pm 0.04) \times 10^{-3}$
70–110	0.32	0.28	0.09	0.68	0.25	0.12	0.34	0.02	1.97	2.17	2.03	$(5.39 \pm 0.16) \times 10^{-4}$
110–150	0.36	0.40	0.12	0.68	0.14	0.15	0.44	0.02	4.32	4.44	4.11	$(1.30 \pm 0.08) \times 10^{-4}$
150–190	0.39	0.49	0.15	0.70	0.62	0.16	0.53	0.02	3.07	3.32	7.89	$(4.21 \pm 0.36) \times 10^{-5}$
190–250	0.41	0.55	0.17	0.71	0.67	0.17	0.61	0.02	5.46	5.62	12.69	$(1.40 \pm 0.19) \times 10^{-5}$
250–600	0.44	0.58	0.18	0.72	0.67	0.18	0.66	0.02	4.94	5.14	19.67	$(1.15 \pm 0.23) \times 10^{-6}$

Table 3. The W boson normalized differential cross sections for the muon channel in bins of $p_{\mathrm{T}}^{\mathrm{W}}$, $(1/\sigma)(\mathrm{d}\sigma/\mathrm{d}p_{\mathrm{T}})$ ($\mathrm{W} \to \mu\nu$), and systematic uncertainties from various sources in units of %. Other details are the same as in table 2.

ref. [60]. The resulting spectra for the W boson normalized differential cross section are shown in figure 4.

POWHEG with PYTHIA using the Z2* tune shows good agreement with the data in the low- and high-$p_{\mathrm{T}}^{\mathrm{W}}$ regions, but overestimates the yield by up to 12% in the transition region at around 25 GeV.

RESBOS-P expectations are consistent with the data for $12.5 < p_{\mathrm{T}}^{\mathrm{W}} < 110$ GeV. Yields are underpredicted for $7.5 < p_{\mathrm{T}}^{\mathrm{W}} < 12.5$ GeV. Above 110 GeV, the predictions systematically overestimate the data by approximately 20%.

JHEP02(2017)096

Bin (GeV)	Bkg.	Muon recon.	Mom. res.	Unfld. bias	FSR	Total syst.	Stat.	$(1/\sigma)(\mathrm{d}\sigma/\mathrm{d}p_{\mathrm{T}})$ (GeV^{-1})
0–2.5	0.43	0.01	0.02	2.71	0.03	2.74	5.53	$(3.34 \pm 0.21) \times 10^{-2}$
2.5–5	0.42	0.00	0.02	1.32	0.02	1.38	4.59	$(5.53 \pm 0.26) \times 10^{-2}$
5–7.5	0.41	0.00	0.01	0.28	0.01	0.50	4.79	$(5.19 \pm 0.25) \times 10^{-2}$
7.5–10	0.29	0.00	0.01	1.30	0.01	1.34	5.78	$(3.86 \pm 0.23) \times 10^{-2}$
10–12.5	0.29	0.00	0.01	1.43	0.01	1.46	5.91	$(3.55 \pm 0.22) \times 10^{-2}$
12.5–15	0.23	0.00	0.00	2.31	0.03	2.33	7.52	$(2.41 \pm 0.19) \times 10^{-2}$
15–17.5	0.15	0.00	0.02	1.29	0.02	1.30	7.59	$(2.25 \pm 0.17) \times 10^{-2}$
17.5–20	0.22	0.00	0.01	1.63	0.04	1.65	8.88	$(1.72 \pm 0.15) \times 10^{-2}$
20–30	0.01	0.00	0.01	0.41	0.02	0.41	4.08	$(1.17 \pm 0.05) \times 10^{-2}$
30–40	0.37	0.00	0.01	0.56	0.00	0.67	5.49	$(6.51 \pm 0.36) \times 10^{-3}$
40–50	0.78	0.00	0.01	1.03	0.01	1.29	7.09	$(4.02 \pm 0.29) \times 10^{-3}$
50–70	1.54	0.00	0.01	0.26	0.02	1.56	6.51	$(2.16 \pm 0.14) \times 10^{-3}$
70–90	2.70	0.00	0.03	0.37	0.04	2.72	10.43	$(8.89 \pm 0.96) \times 10^{-4}$
90–110	3.51	0.00	0.05	0.67	0.01	3.57	15.67	$(4.10 \pm 0.66) \times 10^{-4}$
110–150	3.54	0.00	0.05	1.14	0.13	3.72	16.74	$(1.65 \pm 0.28) \times 10^{-4}$
150–190	2.00	0.01	0.01	0.14	0.18	2.01	24.67	$(7.65 \pm 1.89) \times 10^{-5}$
190–250	6.13	0.01	0.14	9.91	0.33	11.66	68.85	$(8.98 \pm 6.27) \times 10^{-6}$
250–600	2.03	0.00	0.04	0.45	0.23	2.09	44.11	$(4.44 \pm 1.96) \times 10^{-6}$

Table 4. The Z boson normalized differential cross sections for the muon channel in bins of $p_{\mathrm{T}}^{\mathrm{Z}}$, $(1/\sigma)(\mathrm{d}\sigma/\mathrm{d}p_{\mathrm{T}})$ ($\mathrm{Z} \to \mu^+\mu^-$), and systematic uncertainties from various sources in units of %. Other details are the same as in table 2.

FEWZ calculates the cross section for gauge boson production at hadron colliders through order $\mathcal{O}(\alpha_s^2)$ in perturbative QCD. The $p_{\mathrm{T}}^{\mathrm{W}}$ distribution is generated by FEWZ using perturbative QCD at NNLO. The CT10 NNLO PDF set is used with dynamic renormalization and factorization scales set to the value of $\sqrt{M_{\mathrm{W}}^2 + (p_{\mathrm{T}}^{\mathrm{W}})^2}$. The uncertainty of the CT10 PDF set is numerically propagated through FEWZ generation. Scale variations by factors of 1/2 and 2 are applied to estimate the uncertainty. The predictions of FEWZ are in agreement with the data across the whole range in $p_{\mathrm{T}}^{\mathrm{W}}$ within large theoretical uncertainties, except around 60 GeV where it shows 10% discrepancy.

The results for the Z boson differential cross section are presented in figure 5. The RESBOS-CP prediction shows good agreement with data in the accessible region of $p_{\mathrm{T}}^{\mathrm{Z}}$, whereas POWHEG shows 30% lower expectation in the range 0–2.5 GeV and 18% excess for the interval 7.5–10 GeV. As anticipated, the FEWZ prediction with fixed-order perturbation theory shows divergent behavior in the low $p_{\mathrm{T}}^{\mathrm{Z}}$ bins ($p_{\mathrm{T}}^{\mathrm{Z}} \lesssim 20$ GeV). A self-consistent test of FEWZ generation is fulfilled by cross section comparison of the low, high, and full $p_{\mathrm{T}}^{\mathrm{Z}}$ region of the measurement. The ratio of the sum of 0–20 and 20–600 GeV to 0–600 GeV

JHEP02(2017)096

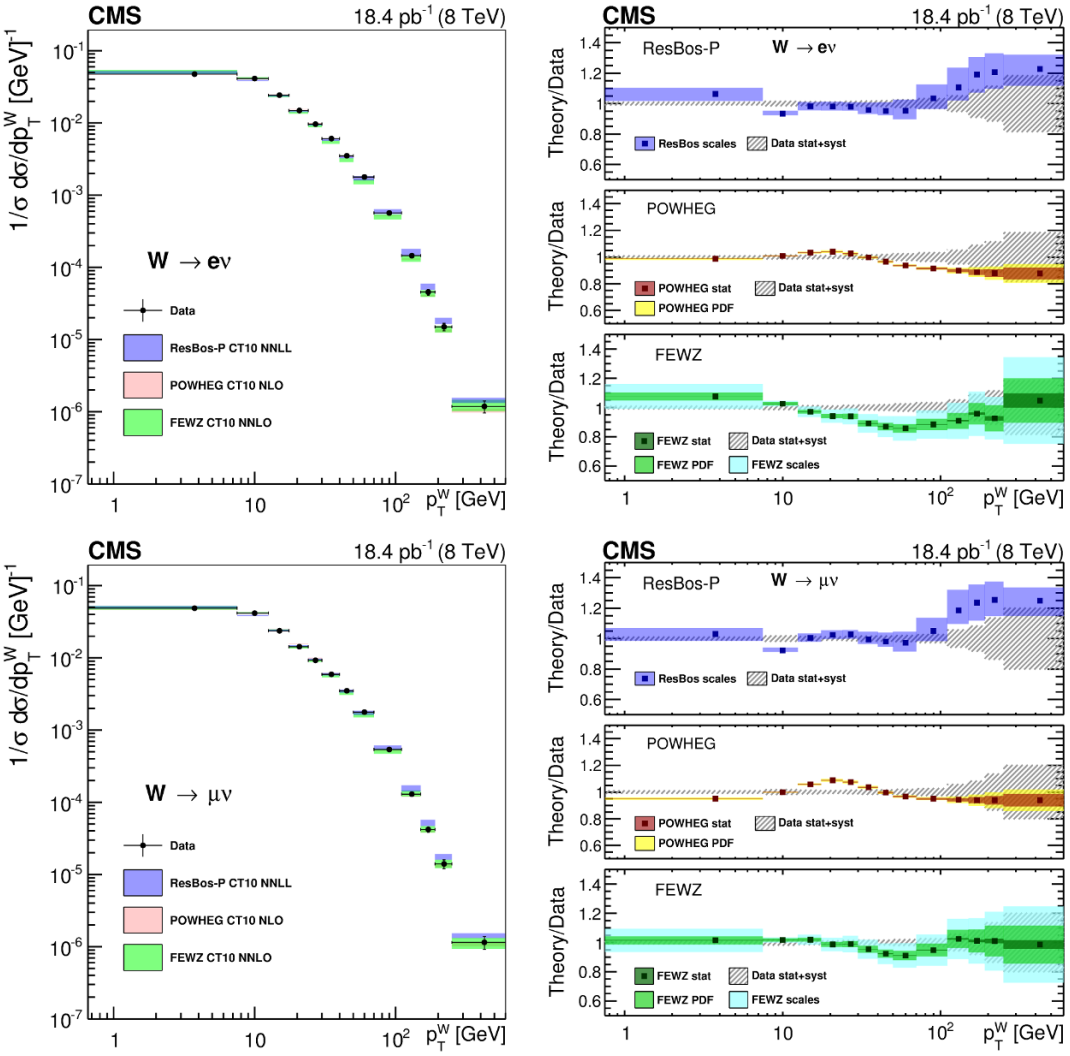

Figure 4. Normalized differential cross sections for charge independent W boson production at the lepton pre-FSR level as a function of $p_{\mathrm{T}}^{\mathrm{W}}$ for electron (upper) and muon (lower) decay channels. The right panels show the ratios of theory predictions to the data. The bands include (i) the statistical uncertainties, uncertainties from scales, and PDF uncertainties for FEWZ; (ii) the statistical uncertainties and PDF uncertainties for POWHEG; (iii) the uncertainty from scales for ResBos-P; and (iv) the sum of the statistical and systematic uncertainties in quadrature for data.

is unity within 10% uncertainty. The ratio of the expectation to data at 0–20 GeV is $1.02 \pm 2.6\%(\textsc{fewz}) \pm 1.1\%\,(\text{data})$.

8.2 Ratios of the cross sections

The ratios of the measured cross sections provide a powerful test of the accuracy of different theoretical predictions because of full or partial cancellation of theoretical uncertainties. The ratio of the normalized spectra corresponding to $\mathrm{W}^- \to \mu^-\overline{\nu}$ and $\mathrm{W}^+ \to \mu^+\nu$ decays is shown in figure 6. The statistical uncertainties in different $p_{\mathrm{T}}^{\mathrm{V}}$ bins are considered to be uncorrelated. The systematic uncertainties are calculated by the method described in

JHEP02(2017)096

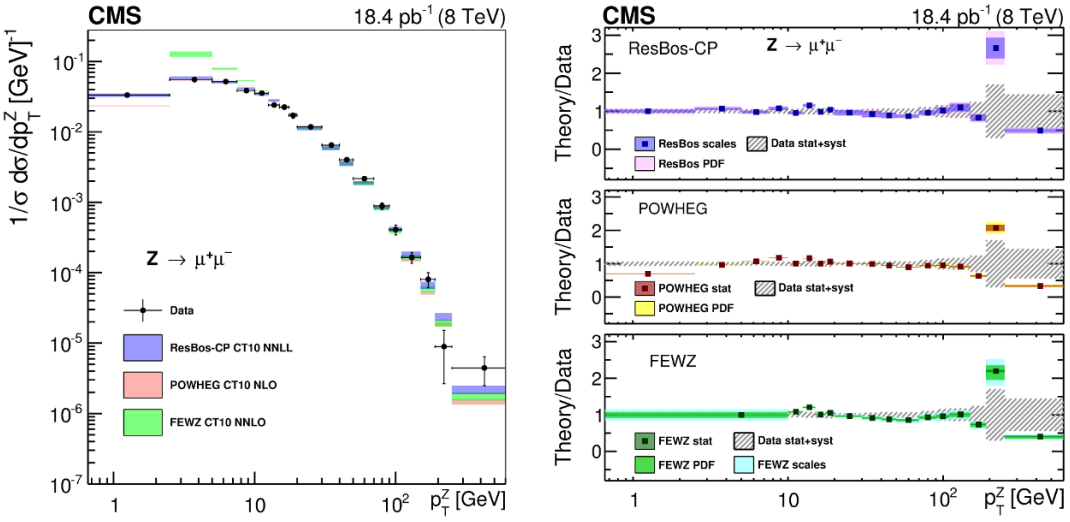

Figure 5. Comparison of the normalized dimuon differential transverse momentum distribution from data (solid symbols) with different theoretical predictions. The right panels show the ratios of theory predictions to the data. The RESBOS-CP version with scale and PDF variation is used for comparison.

section 7 taking into account all correlations between charge-dependent W boson cross sections. The ratios with the total uncertainty are listed in table 5. The results are compared to POWHEG, RESBOS, and FEWZ predictions. The predictions describe the data reasonably well within experimental uncertainties.

The ratio of differential production cross sections for Z to those for W in the muon channel is shown in figure 7 where the total uncertainties of the measurements are considered to be uncorrelated. The ratios with the total uncertainty are listed in table 5. The POWHEG calculation shows good agreement with the data in the low- and high-$p_{\mathrm{T}}^{\mathrm{V}}$ regions, but overestimates the ratio by up to 10% in the transition region at around $p_{\mathrm{T}}^{\mathrm{V}} = 10\,\mathrm{GeV}$. The RESBOS expectation also shows behavior similar to POWHEG, but it has larger than expected uncertainties because it employs different strategies in terms of the scale and PDF variations for the W and Z boson generation, which technically results in no cancellation for their ratio. FEWZ predictions describe the data well for $p_{\mathrm{T}}^{\mathrm{V}} > 20\,\mathrm{GeV}$.

In figure 8 the ratio of differential cross sections for the Z boson production measured at two different centre-of-mass energies, 7 and 8 TeV [18], are shown for the muon channel, separately for low- and high-$p_{\mathrm{T}}^{\mathrm{Z}}$ regions. The theoretical predictions describe the data well within the experimental uncertainties.

9 Summary

The production cross sections of the weak vector bosons, W and Z, as a function of transverse momentum, are measured by the CMS experiment using a sample of proton-proton collisions during a special low luminosity running of the LHC at $\sqrt{s} = 8\,\mathrm{TeV}$ that corresponds to an integrated luminosity of $18.4\,\mathrm{pb}^{-1}$. The production of W bosons is analyzed

JHEP02(2017)096

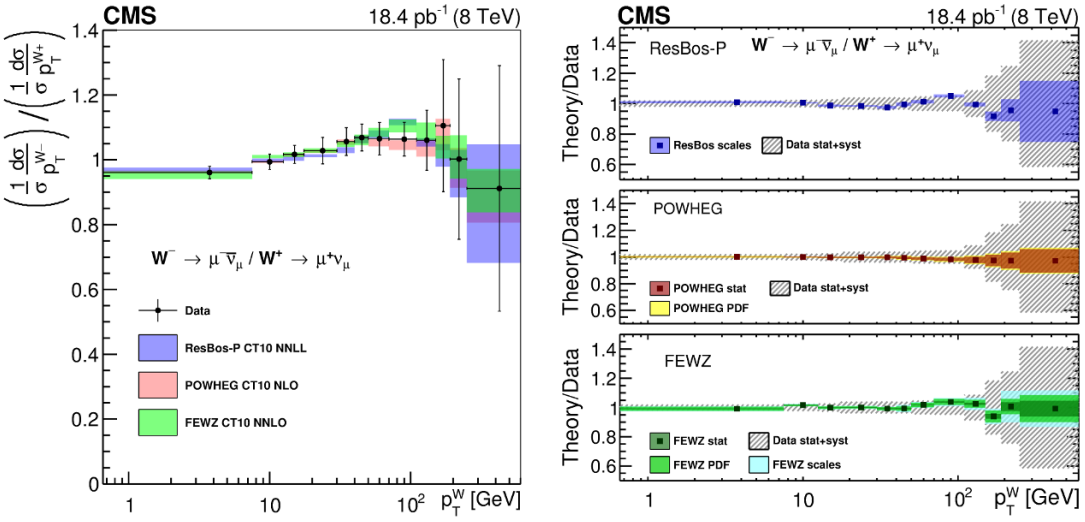

Figure 6. The normalized p_{T} differential cross section ratio of W^- to W^+ for muon channel compared with theoretical predictions. Data points include the sum of the statistical and systematic uncertainties in quadrature. More details are given in the figure 4 caption.

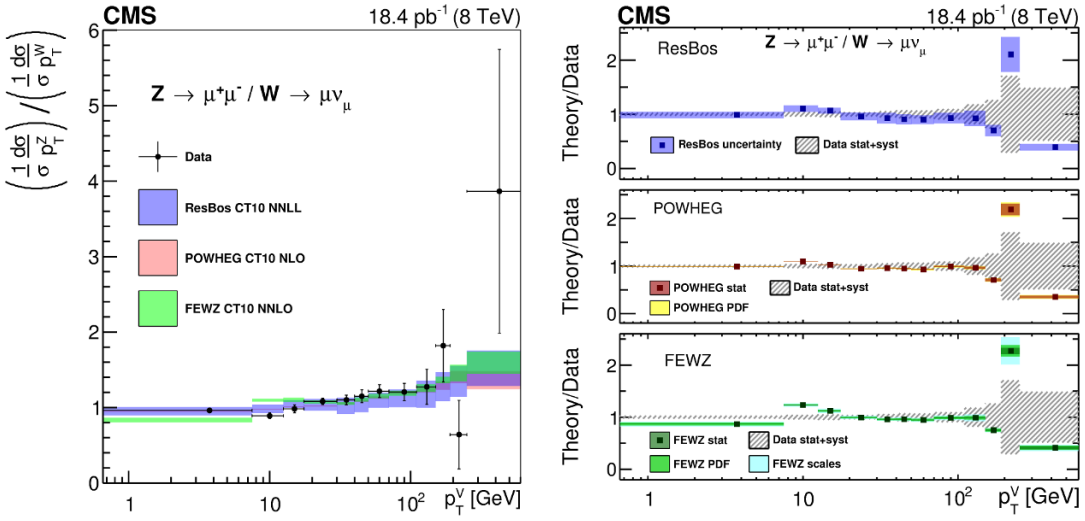

Figure 7. The normalized p_{T} differential cross section ratio of Z to W for muon channel compared with theoretical predictions. The right panels show the ratios of theory predictions to the data. The larger than expected uncertainties for ResBos arise from the different strategies in terms of the scale and PDF variations between ResBos-P and ResBos-CP version. More details are given in the figure 4 and 5 caption.

in both electron and muon decay modes, while the production of Z bosons is analyzed using only the dimuon decay channel.

The measured normalized cross sections are compared to various theoretical predictions. All the predictions provide reasonable descriptions of the data, but POWHEG at NLO overestimates the yield by up to 12% around $p_{\mathrm{T}}^{\mathrm{W}} = 25\,\mathrm{GeV}$. POWHEG shows 27% lower expectation in the $p_{\mathrm{T}}^{\mathrm{Z}}$ range 0–2.5 GeV and 18% excess for the $p_{\mathrm{T}}^{\mathrm{Z}}$ interval 7.5–10 GeV.

JHEP02(2017)096

Bin (GeV)	W^-/W^+	Z/W
0–7.5	0.961 ± 0.019	0.962 ± 0.025
7.5–12.5	0.994 ± 0.024	0.890 ± 0.038
12.5–17.5	1.017 ± 0.028	0.982 ± 0.052
17.5–30	1.028 ± 0.041	1.081 ± 0.041
30–40	1.056 ± 0.043	1.101 ± 0.064
40–50	1.069 ± 0.041	1.149 ± 0.085
50–70	1.065 ± 0.050	1.216 ± 0.085
70–110	1.064 ± 0.052	1.206 ± 0.115
110–150	1.061 ± 0.093	1.274 ± 0.232
150–190	1.106 ± 0.204	1.820 ± 0.479
190–250	1.002 ± 0.247	0.641 ± 0.454
250–600	0.912 ± 0.379	3.865 ± 1.881

Table 5. Estimated ratios of pre-FSR level normalized differential cross sections within the muon fiducial volume. The uncertainty is the sum of statistical and systematic uncertainties in quadrature.

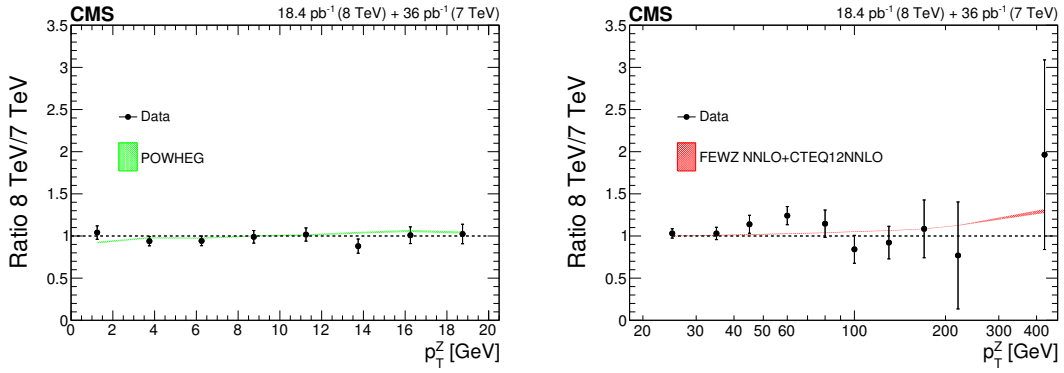

Figure 8. Comparison of the shapes of the differential p_T^Z distributions in the muon channel at centre-of-mass energies of 7 and 8 TeV compared with the predictions from POWHEG for $p_T^Z < 20$ GeV and FEWZ for $p_T^Z > 20$ GeV.

FEWZ at NNLO shows 10% discrepancy around $p_T^W = 60$ GeV and divergent behavior in the low p_T^Z region where bin widths are finer than those of the W boson study. RESBOS-P systematically overestimates the cross section by approximately 20% above $p_T^W = 110$ GeV, but the CP version demonstrates good agreement with data in the accessible region of p_T^Z. The ratios of W^- to W^+, Z to W boson differential cross sections, as well as the ratio of Z boson production cross sections at centre-of-mass energies 7 to 8 TeV are calculated to allow for more precise comparisons with data. Overall, the different theoretical models describe the ratios well.

JHEP02(2017)096

Acknowledgments

We congratulate our colleagues in the CERN accelerator departments for the excellent performance of the LHC and thank the technical and administrative staffs at CERN and at other CMS institutes for their contributions to the success of the CMS effort. In addition, we gratefully acknowledge the computing centres and personnel of the Worldwide LHC Computing Grid for delivering so effectively the computing infrastructure essential to our analyses. Finally, we acknowledge the enduring support for the construction and operation of the LHC and the CMS detector provided by the following funding agencies: the Austrian Federal Ministry of Science, Research and Economy and the Austrian Science Fund; the Belgian Fonds de la Recherche Scientifique, and Fonds voor Wetenschappelijk Onderzoek; the Brazilian Funding Agencies (CNPq, CAPES, FAPERJ, and FAPESP); the Bulgarian Ministry of Education and Science; CERN; the Chinese Academy of Sciences, Ministry of Science and Technology, and National Natural Science Foundation of China; the Colombian Funding Agency (COLCIENCIAS); the Croatian Ministry of Science, Education and Sport, and the Croatian Science Foundation; the Research Promotion Foundation, Cyprus; the Secretariat for Higher Education, Science, Technology and Innovation, Ecuador; the Ministry of Education and Research, Estonian Research Council via IUT23-4 and IUT23-6 and European Regional Development Fund, Estonia; the Academy of Finland, Finnish Ministry of Education and Culture, and Helsinki Institute of Physics; the Institut National de Physique Nucléaire et de Physique des Particules / CNRS, and Commissariat à l'Énergie Atomique et aux Énergies Alternatives / CEA, France; the Bundesministerium für Bildung und Forschung, Deutsche Forschungsgemeinschaft, and Helmholtz-Gemeinschaft Deutscher Forschungszentren, Germany; the General Secretariat for Research and Technology, Greece; the National Scientific Research Foundation, and National Innovation Office, Hungary; the Department of Atomic Energy and the Department of Science and Technology, India; the Institute for Studies in Theoretical Physics and Mathematics, Iran; the Science Foundation, Ireland; the Istituto Nazionale di Fisica Nucleare, Italy; the Ministry of Science, ICT and Future Planning, and National Research Foundation (NRF), Republic of Korea; the Lithuanian Academy of Sciences; the Ministry of Education, and University of Malaya (Malaysia); the Mexican Funding Agencies (BUAP, CINVESTAV, CONACYT, LNS, SEP, and UASLP-FAI); the Ministry of Business, Innovation and Employment, New Zealand; the Pakistan Atomic Energy Commission; the Ministry of Science and Higher Education and the National Science Centre, Poland; the Fundação para a Ciência e a Tecnologia, Portugal; JINR, Dubna; the Ministry of Education and Science of the Russian Federation, the Federal Agency of Atomic Energy of the Russian Federation, Russian Academy of Sciences, and the Russian Foundation for Basic Research; the Ministry of Education, Science and Technological Development of Serbia; the Secretaría de Estado de Investigación, Desarrollo e Innovación and Programa Consolider-Ingenio 2010, Spain; the Swiss Funding Agencies (ETH Board, ETH Zurich, PSI, SNF, UniZH, Canton Zurich, and SER); the Ministry of Science and Technology, Taipei; the Thailand Center of Excellence in Physics, the Institute for the Promotion of Teaching Science and Technology of Thailand, Special Task Force for Activating Research and the National Science and Technology Development

JHEP02(2017)096

Agency of Thailand; the Scientific and Technical Research Council of Turkey, and Turkish Atomic Energy Authority; the National Academy of Sciences of Ukraine, and State Fund for Fundamental Researches, Ukraine; the Science and Technology Facilities Council, U.K.; the US Department of Energy, and the US National Science Foundation.

Individuals have received support from the Marie-Curie programme and the European Research Council and EPLANET (European Union); the Leventis Foundation; the A. P. Sloan Foundation; the Alexander von Humboldt Foundation; the Belgian Federal Science Policy Office; the Fonds pour la Formation à la Recherche dans l'Industrie et dans l'Agriculture (FRIA-Belgium); the Agentschap voor Innovatie door Wetenschap en Technologie (IWT-Belgium); the Ministry of Education, Youth and Sports (MEYS) of the Czech Republic; the Council of Science and Industrial Research, India; the HOMING PLUS programme of the Foundation for Polish Science, cofinanced from European Union, Regional Development Fund, the Mobility Plus programme of the Ministry of Science and Higher Education, the OPUS programme contract 2014/13/B/ST2/02543 and contract Sonata-bis DEC-2012/07/E/ST2/01406 of the National Science Center (Poland); Kyungpook National University Research Fund (2014) (Republic of Korea); the Thalis and Aristeia programmes cofinanced by EU-ESF and the Greek NSRF; the National Priorities Research Program by Qatar National Research Fund; the Programa Clarín-COFUND del Principado de Asturias; the Rachadapisek Sompot Fund for Postdoctoral Fellowship, Chulalongkorn University and the Chulalongkorn Academic into Its 2nd Century Project Advancement Project (Thailand); and the Welch Foundation, contract C-1845.

JHEP02(2017)096

References

[1] C. Balázs and C.P. Yuan, *Soft gluon effects on lepton pairs at hadron colliders*, *Phys. Rev.* **D 56** (1997) 5558 [hep-ph/9704258] [INSPIRE].

[2] K. Melnikov and F. Petriello, *Electroweak gauge boson production at hadron colliders through* $O(\alpha_s^2)$, *Phys. Rev.* **D 74** (2006) 114017 [hep-ph/0609070] [INSPIRE].

[3] CMS collaboration, *Measurement of inclusive W and Z boson production cross sections in pp collisions at* $\sqrt{s} = 8$ *TeV*, *Phys. Rev. Lett.* **112** (2014) 191802 [arXiv:1402.0923] [INSPIRE].

[4] CMS collaboration, *Measurement of the Z boson differential cross section in transverse momentum and rapidity in proton-proton collisions at* 8 *TeV*, *Phys. Lett.* **B 749** (2015) 187 [arXiv:1504.03511] [INSPIRE].

[5] CDF collaboration, F. Abe et al., *Measurement of the W* p_T *distribution in* $\bar{p}p$ *collisions at* $\sqrt{s} = 1.8$ *TeV*, *Phys. Rev. Lett.* **66** (1991) 2951 [INSPIRE].

[6] D0 collaboration, B. Abbott et al., *Measurement of the shape of the transverse momentum distribution of W bosons produced in* $p\bar{p}$ *collisions at* $\sqrt{s} = 1.8$ *TeV*, *Phys. Rev. Lett.* **80** (1998) 5498 [hep-ex/9803003] [INSPIRE].

[7] CDF collaboration, A. Abulencia et al., *Measurements of inclusive W and Z cross sections in $p\bar{p}$ collisions at $\sqrt{s} = 1.96$ TeV*, *J. Phys.* **G 34** (2007) 2457 [hep-ex/0508029] [INSPIRE].

[8] D0 collaboration, V.M. Abazov et al., *Measurement of differential Z/γ^* + jet + X cross sections in $p\bar{p}$ collisions at $\sqrt{s} = 1.96$ TeV*, *Phys. Lett.* **B 669** (2008) 278 [arXiv:0808.1296] [INSPIRE].

[9] D0 collaboration, V.M. Abazov et al., *Measurement of the shape of the boson transverse momentum distribution in $p\bar{p} \to Z/\gamma^* \to e^+e^- + X$ events produced at $\sqrt{s} = 1.96$ TeV*, *Phys. Rev. Lett.* **100** (2008) 102002 [arXiv:0712.0803] [INSPIRE].

[10] D0 collaboration, V.M. Abazov et al., *Measurement of the normalized $Z/\gamma^* \to \mu^+\mu^-$ transverse momentum distribution in $p\bar{p}$ collisions at $\sqrt{s} = 1.96$ TeV*, *Phys. Lett.* **B 693** (2010) 522 [arXiv:1006.0618] [INSPIRE].

[11] D0 collaboration, V.M. Abazov et al., *Precise study of the Z/γ^* boson transverse momentum distribution in $p\bar{p}$ collisions using a novel technique*, *Phys. Rev. Lett.* **106** (2011) 122001 [arXiv:1010.0262] [INSPIRE].

[12] ATLAS collaboration, *Measurement of the inclusive $W^\pm$ and Z/γ cross sections in the electron and muon decay channels in pp collisions at $\sqrt{s} = 7$ TeV with the ATLAS detector*, *Phys. Rev.* **D 85** (2012) 072004 [arXiv:1109.5141] [INSPIRE].

[13] CMS collaboration, *Measurement of the inclusive W and Z production cross sections in pp collisions at $\sqrt{s} = 7$ TeV*, *JHEP* **10** (2011) 132 [arXiv:1107.4789] [INSPIRE].

[14] CMS collaboration, *Measurement of the differential and double-differential Drell-Yan cross sections in proton-proton collisions at $\sqrt{s} = 7$ TeV*, *JHEP* **12** (2013) 030 [arXiv:1310.7291] [INSPIRE].

[15] CMS collaboration, *Measurements of differential and double-differential Drell-Yan cross sections in proton-proton collisions at 8 TeV*, *Eur. Phys. J.* **C 75** (2015) 147 [arXiv:1412.1115] [INSPIRE].

[16] ATLAS collaboration, *Measurement of the transverse momentum distribution of Z/γ^* bosons in proton-proton collisions at $\sqrt{s} = 7$ TeV with the ATLAS detector*, *Phys. Lett.* **B 705** (2011) 415 [arXiv:1107.2381] [INSPIRE].

[17] ATLAS collaboration, *Measurement of the Z/γ^* boson transverse momentum distribution in pp collisions at $\sqrt{s} = 7$ TeV with the ATLAS detector*, *JHEP* **09** (2014) 145 [arXiv:1406.3660] [INSPIRE].

[18] CMS collaboration, *Measurement of the rapidity and transverse momentum distributions of Z bosons in pp collisions at $\sqrt{s} = 7$ TeV*, *Phys. Rev.* **D 85** (2012) 032002 [arXiv:1110.4973] [INSPIRE].

[19] ATLAS collaboration, *Measurement of the transverse momentum distribution of W bosons in pp collisions at $\sqrt{s} = 7$ TeV with the ATLAS detector*, *Phys. Rev.* **D 85** (2012) 012005 [arXiv:1108.6308] [INSPIRE].

[20] LHCb collaboration, *Inclusive W and Z production in the forward region at $\sqrt{s} = 7$ TeV*, *JHEP* **06** (2012) 058 [arXiv:1204.1620] [INSPIRE].

[21] LHCb collaboration, *Measurement of the cross-section for $Z \to e^+e^-$ production in pp collisions at $\sqrt{s} = 7$ TeV*, *JHEP* **02** (2013) 106 [arXiv:1212.4620] [INSPIRE].

[22] LHCb collaboration, *A study of the Z production cross-section in pp collisions at $\sqrt{s} = 7$ TeV using tau final states*, *JHEP* **01** (2013) 111 [arXiv:1210.6289] [INSPIRE].

JHEP02(2017)096

[23] LHCb collaboration, *Measurement of the forward Z boson production cross-section in pp collisions at $\sqrt{s} = 7$ TeV*, *JHEP* **08** (2015) 039 [arXiv:1505.07024] [INSPIRE].

[24] LHCb collaboration, *Measurement of the forward W boson cross-section in pp collisions at $\sqrt{s} = 7$ TeV*, *JHEP* **12** (2014) 079 [arXiv:1408.4354] [INSPIRE].

[25] LHCb collaboration, *Measurement of forward W and Z boson production in pp collisions at $\sqrt{s} = 8$ TeV*, *JHEP* **01** (2016) 155 [arXiv:1511.08039] [INSPIRE].

[26] C. Anastasiou, L.J. Dixon, K. Melnikov and F. Petriello, *High precision QCD at hadron colliders: Electroweak gauge boson rapidity distributions at NNLO*, *Phys. Rev.* **D 69** (2004) 094008 [hep-ph/0312266] [INSPIRE].

[27] R. Gavin, Y. Li, F. Petriello and S. Quackenbush, *FEWZ 2.0: a code for hadronic Z production at next-to-next-to-leading order*, *Comput. Phys. Commun.* **182** (2011) 2388 [arXiv:1011.3540] [INSPIRE].

[28] R. Gavin, Y. Li, F. Petriello and S. Quackenbush, *W Physics at the LHC with FEWZ 2.1*, *Comput. Phys. Commun.* **184** (2013) 208 [arXiv:1201.5896] [INSPIRE].

[29] Y. Li and F. Petriello, *Combining QCD and electroweak corrections to dilepton production in FEWZ*, *Phys. Rev.* **D 86** (2012) 094034 [arXiv:1208.5967] [INSPIRE].

[30] G.A. Ladinsky and C.P. Yuan, *The Nonperturbative regime in QCD resummation for gauge boson production at hadron colliders*, *Phys. Rev.* **D 50** (1994) R4239 [hep-ph/9311341] [INSPIRE].

[31] F. Landry, R. Brock, P.M. Nadolsky and C.P. Yuan, *Tevatron Run-1 Z boson data and Collins-Soper-Sterman resummation formalism*, *Phys. Rev.* **D 67** (2003) 073016 [hep-ph/0212159] [INSPIRE].

[32] M. Guzzi, P.M. Nadolsky and B. Wang, *Nonperturbative contributions to a resummed leptonic angular distribution in inclusive neutral vector boson production*, *Phys. Rev.* **D 90** (2014) 014030 [arXiv:1309.1393] [INSPIRE].

[33] S. Frixione, P. Nason and C. Oleari, *Matching NLO QCD computations with Parton Shower simulations: the POWHEG method*, *JHEP* **11** (2007) 070 [arXiv:0709.2092] [INSPIRE].

[34] P. Nason, *A new method for combining NLO QCD with shower Monte Carlo algorithms*, *JHEP* **11** (2004) 040 [hep-ph/0409146] [INSPIRE].

[35] S. Alioli, P. Nason, C. Oleari and E. Re, *NLO vector-boson production matched with shower in POWHEG*, *JHEP* **07** (2008) 060 [arXiv:0805.4802] [INSPIRE].

[36] S. Alioli, P. Nason, C. Oleari and E. Re, *A general framework for implementing NLO calculations in shower Monte Carlo programs: the POWHEG BOX*, *JHEP* **06** (2010) 043 [arXiv:1002.2581] [INSPIRE].

[37] T. Sjöstrand, S. Mrenna and P.Z. Skands, *PYTHIA 6.4 physics and manual*, *JHEP* **05** (2006) 026 [hep-ph/0603175] [INSPIRE].

[38] CMS collaboration, *The CMS experiment at the CERN LHC*, 2008 *JINST* **3** S08004 [INSPIRE].

[39] H.-L. Lai et al., *New parton distributions for collider physics*, *Phys. Rev.* **D 82** (2010) 074024 [arXiv:1007.2241] [INSPIRE].

[40] J. Alwall, M. Herquet, F. Maltoni, O. Mattelaer and T. Stelzer, *MadGraph 5: going beyond*, *JHEP* **06** (2011) 128 [arXiv:1106.0522] [INSPIRE].

JHEP02(2017)096

[41] R. Field, *Early LHC underlying event data — Findings and surprises*, arXiv:1010.3558 [INSPIRE].

[42] J. Pumplin, D.R. Stump, J. Huston, H.L. Lai, P.M. Nadolsky and W.K. Tung, *New generation of parton distributions with uncertainties from global QCD analysis*, *JHEP* **07** (2002) 012 [hep-ph/0201195] [INSPIRE].

[43] F. Maltoni and T. Stelzer, *MadEvent: automatic event generation with MadGraph*, *JHEP* **02** (2003) 027 [hep-ph/0208156] [INSPIRE].

[44] GEANT4 collaboration, S. Agostinelli et al., *GEANT4 — A simulation toolkit*, *Nucl. Instrum. Meth.* **A 506** (2003) 250 [INSPIRE].

[45] CMS collaboration, *Particle-flow event reconstruction in CMS and performance for jets, taus and MET*, CMS-PAS-PFT-09-001 (2009).

[46] CMS collaboration, *Commissioning of the particle-flow event reconstruction with the first LHC collisions recorded in the CMS detector*, CMS-PAS-PFT-10-001 (2010).

[47] W. Adam, R. Frühwirth, A. Strandlie and T. Todorov, *Reconstruction of electrons with the Gaussian sum filter in the CMS tracker at LHC*, *eConf* **C 0303241** (2003) TULT009 [physics/0306087] [INSPIRE].

[48] CMS collaboration, *Performance of electron reconstruction and selection with the CMS detector in proton-proton collisions at* $\sqrt{s} = 8$ *TeV*, 2015 *JINST* **10** P06005 [arXiv:1502.02701] [INSPIRE].

[49] CMS collaboration, *Performance of photon reconstruction and identification with the CMS detector in proton-proton collisions at* $\sqrt{s} = 8$ *TeV*, 2015 *JINST* **10** P08010 [arXiv:1502.02702] [INSPIRE].

[50] CMS collaboration, *Performance of CMS muon reconstruction in pp collision events at* $\sqrt{s} = 7$ *TeV*, 2012 *JINST* **7** P10002 [arXiv:1206.4071] [INSPIRE].

[51] M. Cacciari and G.P. Salam, *Pileup subtraction using jet areas*, *Phys. Lett.* **B 659** (2008) 119 [arXiv:0707.1378] [INSPIRE].

[52] CMS collaboration, *Missing transverse energy performance of the CMS detector*, 2011 *JINST* **6** P09001 [arXiv:1106.5048] [INSPIRE].

[53] CMS collaboration, *Measurements of inclusive* W *and* Z *cross sections in pp collisions at* $\sqrt{s} = 7$ *TeV*, *JHEP* **01** (2011) 080 [arXiv:1012.2466] [INSPIRE].

[54] A. Hocker and V. Kartvelishvili, *SVD approach to data unfolding*, *Nucl. Instrum. Meth.* **A 372** (1996) 469 [hep-ph/9509307] [INSPIRE].

[55] V. Blobel, *An unfolding method for high-energy physics experiments*, hep-ex/0208022 [INSPIRE].

[56] G. Nanava and Z. Was, *How to use SANC to improve the PHOTOS Monte Carlo simulation of bremsstrahlung in leptonic W boson decays*, *Acta Phys. Polon.* **B 34** (2003) 4561 [hep-ph/0303260] [INSPIRE].

[57] H. Burkhardt and B. Pietrzyk, *Update of the hadronic contribution to the QED vacuum polarization*, *Phys. Lett.* **B 513** (2001) 46 [INSPIRE].

[58] J.C. Collins and D.E. Soper, *Back-to-back jets in QCD*, *Nucl. Phys.* **B 193** (1981) 381 [*Erratum ibid.* **B 213** (1983) 545] [INSPIRE].

JHEP02(2017)096

[59] J.C. Collins, D.E. Soper and G.F. Sterman, *Transverse momentum distribution in Drell-Yan pair and W and Z boson production*, *Nucl. Phys.* **B 250** (1985) 199 [INSPIRE].

[60] D. Bourilkov, R.C. Group and M.R. Whalley, *LHAPDF: PDF use from the Tevatron to the LHC*, hep-ph/0605240 [INSPIRE].

JHEP02(2017)096

The CMS collaboration

Yerevan Physics Institute, Yerevan, Armenia

V. Khachatryan, A.M. Sirunyan, A. Tumasyan

Institut für Hochenergiephysik der OeAW, Wien, Austria

W. Adam, E. Asilar, T. Bergauer, J. Brandstetter, E. Brondolin, M. Dragicevic, J. Erö, M. Flechl, M. Friedl, R. Frühwirth[1], V.M. Ghete, C. Hartl, N. Hörmann, J. Hrubec, M. Jeitler[1], A. König, M. Krammer[1], I. Krätschmer, D. Liko, T. Matsushita, I. Mikulec, D. Rabady, N. Rad, B. Rahbaran, H. Rohringer, J. Schieck[1], R. Schöfbeck, J. Strauss, W. Treberer-Treberspurg, W. Waltenberger, C.-E. Wulz[1]

National Centre for Particle and High Energy Physics, Minsk, Belarus

V. Mossolov, N. Shumeiko, J. Suarez Gonzalez

Universiteit Antwerpen, Antwerpen, Belgium

S. Alderweireldt, T. Cornelis, E.A. De Wolf, X. Janssen, A. Knutsson, J. Lauwers, S. Luyckx, M. Van De Klundert, H. Van Haevermaet, P. Van Mechelen, N. Van Remortel, A. Van Spilbeeck

Vrije Universiteit Brussel, Brussel, Belgium

S. Abu Zeid, F. Blekman, J. D'Hondt, N. Daci, I. De Bruyn, K. Deroover, N. Heracleous, J. Keaveney, S. Lowette, S. Moortgat, L. Moreels, A. Olbrechts, Q. Python, D. Strom, S. Tavernier, W. Van Doninck, P. Van Mulders, I. Van Parijs

Université Libre de Bruxelles, Bruxelles, Belgium

H. Brun, C. Caillol, B. Clerbaux, G. De Lentdecker, G. Fasanella, L. Favart, R. Goldouzian, A. Grebenyuk, G. Karapostoli, T. Lenzi, A. Léonard, T. Maerschalk, A. Marinov, A. Randle-conde, T. Seva, C. Vander Velde, P. Vanlaer, R. Yonamine, F. Zenoni, F. Zhang[2]

Ghent University, Ghent, Belgium

L. Benucci, A. Cimmino, S. Crucy, D. Dobur, A. Fagot, G. Garcia, M. Gul, J. Mccartin, A.A. Ocampo Rios, D. Poyraz, D. Ryckbosch, S. Salva, M. Sigamani, M. Tytgat, W. Van Driessche, E. Yazgan, N. Zaganidis

Université Catholique de Louvain, Louvain-la-Neuve, Belgium

S. Basegmez, C. Beluffi[3], O. Bondu, S. Brochet, G. Bruno, A. Caudron, L. Ceard, S. De Visscher, C. Delaere, M. Delcourt, D. Favart, L. Forthomme, A. Giammanco, A. Jafari, P. Jez, M. Komm, V. Lemaitre, A. Mertens, M. Musich, C. Nuttens, K. Piotrzkowski, L. Quertenmont, M. Selvaggi, M. Vidal Marono

Université de Mons, Mons, Belgium

N. Beliy, G.H. Hammad

Centro Brasileiro de Pesquisas Fisicas, Rio de Janeiro, Brazil

W.L. Aldá Júnior, F.L. Alves, G.A. Alves, L. Brito, M. Correa Martins Junior, M. Hamer, C. Hensel, A. Moraes, M.E. Pol, P. Rebello Teles

JHEP02(2017)096

Universidade do Estado do Rio de Janeiro, Rio de Janeiro, Brazil

E. Belchior Batista Das Chagas, W. Carvalho, J. Chinellato[4], A. Custódio, E.M. Da Costa, D. De Jesus Damiao, C. De Oliveira Martins, S. Fonseca De Souza, L.M. Huertas Guativa, H. Malbouisson, D. Matos Figueiredo, C. Mora Herrera, L. Mundim, H. Nogima, W.L. Prado Da Silva, A. Santoro, A. Sznajder, E.J. Tonelli Manganote[4], A. Vilela Pereira

Universidade Estadual Paulista [a], Universidade Federal do ABC [b], São Paulo, Brazil

S. Ahuja[a], C.A. Bernardes[b], A. De Souza Santos[b], S. Dogra[a], T.R. Fernandez Perez Tomei[a], E.M. Gregores[b], P.G. Mercadante[b], C.S. Moon[a,5], S.F. Novaes[a], Sandra S. Padula[a], D. Romero Abad[b], J.C. Ruiz Vargas

Institute for Nuclear Research and Nuclear Energy, Sofia, Bulgaria

A. Aleksandrov, R. Hadjiiska, P. Iaydjiev, M. Rodozov, S. Stoykova, G. Sultanov, M. Vutova

University of Sofia, Sofia, Bulgaria

A. Dimitrov, I. Glushkov, L. Litov, B. Pavlov, P. Petkov

Beihang University, Beijing, China

W. Fang[6]

Institute of High Energy Physics, Beijing, China

M. Ahmad, J.G. Bian, G.M. Chen, H.S. Chen, M. Chen, T. Cheng, R. Du, C.H. Jiang, D. Leggat, R. Plestina[7], F. Romeo, S.M. Shaheen, A. Spiezia, J. Tao, C. Wang, Z. Wang, H. Zhang

State Key Laboratory of Nuclear Physics and Technology, Peking University, Beijing, China

C. Asawatangtrakuldee, Y. Ban, Q. Li, S. Liu, Y. Mao, S.J. Qian, D. Wang, Z. Xu

Universidad de Los Andes, Bogota, Colombia

C. Avila, A. Cabrera, L.F. Chaparro Sierra, C. Florez, J.P. Gomez, B. Gomez Moreno, J.C. Sanabria

University of Split, Faculty of Electrical Engineering, Mechanical Engineering and Naval Architecture, Split, Croatia

N. Godinovic, D. Lelas, I. Puljak, P.M. Ribeiro Cipriano

University of Split, Faculty of Science, Split, Croatia

Z. Antunovic, M. Kovac

Institute Rudjer Boskovic, Zagreb, Croatia

V. Brigljevic, D. Ferencek, K. Kadija, J. Luetic, S. Micanovic, L. Sudic

University of Cyprus, Nicosia, Cyprus

A. Attikis, G. Mavromanolakis, J. Mousa, C. Nicolaou, F. Ptochos, P.A. Razis, H. Rykaczewski

JHEP02(2017)096

Charles University, Prague, Czech Republic
M. Finger[8], M. Finger Jr.[8]

Universidad San Francisco de Quito, Quito, Ecuador
E. Carrera Jarrin

Academy of Scientific Research and Technology of the Arab Republic of Egypt, Egyptian Network of High Energy Physics, Cairo, Egypt
A. Awad, S. Elgammal[9], A. Mohamed[10], E. Salama[9,11]

National Institute of Chemical Physics and Biophysics, Tallinn, Estonia
B. Calpas, M. Kadastik, M. Murumaa, L. Perrini, M. Raidal, A. Tiko, C. Veelken

Department of Physics, University of Helsinki, Helsinki, Finland
P. Eerola, J. Pekkanen, M. Voutilainen

Helsinki Institute of Physics, Helsinki, Finland
J. Härkönen, V. Karimäki, R. Kinnunen, T. Lampén, K. Lassila-Perini, S. Lehti, T. Lindén, P. Luukka, T. Peltola, J. Tuominiemi, E. Tuovinen, L. Wendland

Lappeenranta University of Technology, Lappeenranta, Finland
J. Talvitie, T. Tuuva

DSM/IRFU, CEA/Saclay, Gif-sur-Yvette, France
M. Besancon, F. Couderc, M. Dejardin, D. Denegri, B. Fabbro, J.L. Faure, C. Favaro, F. Ferri, S. Ganjour, A. Givernaud, P. Gras, G. Hamel de Monchenault, P. Jarry, E. Locci, M. Machet, J. Malcles, J. Rander, A. Rosowsky, M. Titov, A. Zghiche

Laboratoire Leprince-Ringuet, Ecole Polytechnique, IN2P3-CNRS, Palaiseau, France
A. Abdulsalam, I. Antropov, S. Baffioni, F. Beaudette, P. Busson, L. Cadamuro, E. Chapon, C. Charlot, O. Davignon, R. Granier de Cassagnac, M. Jo, S. Lisniak, P. Miné, I.N. Naranjo, M. Nguyen, C. Ochando, G. Ortona, P. Paganini, P. Pigard, S. Regnard, R. Salerno, Y. Sirois, T. Strebler, Y. Yilmaz, A. Zabi

Institut Pluridisciplinaire Hubert Curien, Université de Strasbourg, Université de Haute Alsace Mulhouse, CNRS/IN2P3, Strasbourg, France
J.-L. Agram[12], J. Andrea, A. Aubin, D. Bloch, J.-M. Brom, M. Buttignol, E.C. Chabert, N. Chanon, C. Collard, E. Conte[12], X. Coubez, J.-C. Fontaine[12], D. Gelé, U. Goerlach, C. Goetzmann, A.-C. Le Bihan, J.A. Merlin[13], K. Skovpen, P. Van Hove

Centre de Calcul de l'Institut National de Physique Nucleaire et de Physique des Particules, CNRS/IN2P3, Villeurbanne, France
S. Gadrat

Université de Lyon, Université Claude Bernard Lyon 1, CNRS-IN2P3, Institut de Physique Nucléaire de Lyon, Villeurbanne, France
S. Beauceron, C. Bernet, G. Boudoul, E. Bouvier, C.A. Carrillo Montoya, R. Chierici, D. Contardo, B. Courbon, P. Depasse, H. El Mamouni, J. Fan, J. Fay, S. Gascon, M. Gouze-

JHEP02(2017)096

vitch, B. Ille, F. Lagarde, I.B. Laktineh, M. Lethuillier, L. Mirabito, A.L. Pequegnot, S. Perries, A. Popov[14], J.D. Ruiz Alvarez, D. Sabes, V. Sordini, M. Vander Donckt, P. Verdier, S. Viret

Georgian Technical University, Tbilisi, Georgia
A. Khvedelidze[8]

Tbilisi State University, Tbilisi, Georgia
Z. Tsamalaidze[8]

RWTH Aachen University, I. Physikalisches Institut, Aachen, Germany
C. Autermann, S. Beranek, L. Feld, A. Heister, M.K. Kiesel, K. Klein, M. Lipinski, A. Ostapchuk, M. Preuten, F. Raupach, S. Schael, J.F. Schulte, T. Verlage, H. Weber, V. Zhukov[14]

RWTH Aachen University, III. Physikalisches Institut A, Aachen, Germany
M. Ata, M. Brodski, E. Dietz-Laursonn, D. Duchardt, M. Endres, M. Erdmann, S. Erdweg, T. Esch, R. Fischer, A. Güth, T. Hebbeker, C. Heidemann, K. Hoepfner, S. Knutzen, M. Merschmeyer, A. Meyer, P. Millet, S. Mukherjee, M. Olschewski, K. Padeken, P. Papacz, T. Pook, M. Radziej, H. Reithler, M. Rieger, F. Scheuch, L. Sonnenschein, D. Teyssier, S. Thüer

RWTH Aachen University, III. Physikalisches Institut B, Aachen, Germany
V. Cherepanov, Y. Erdogan, G. Flügge, H. Geenen, M. Geisler, F. Hoehle, B. Kargoll, T. Kress, A. Künsken, J. Lingemann, A. Nehrkorn, A. Nowack, I.M. Nugent, C. Pistone, O. Pooth, A. Stahl[13]

Deutsches Elektronen-Synchrotron, Hamburg, Germany
M. Aldaya Martin, I. Asin, K. Beernaert, O. Behnke, U. Behrens, K. Borras[15], A. Burgmeier, A. Campbell, C. Contreras-Campana, F. Costanza, C. Diez Pardos, G. Dolinska, S. Dooling, G. Eckerlin, D. Eckstein, T. Eichhorn, E. Gallo[16], J. Garay Garcia, A. Geiser, A. Gizhko, P. Gunnellini, A. Harb, J. Hauk, M. Hempel[17], H. Jung, A. Kalogeropoulos, O. Karacheban[17], M. Kasemann, P. Katsas, J. Kieseler, C. Kleinwort, I. Korol, W. Lange, J. Leonard, K. Lipka, A. Lobanov, W. Lohmann[17], R. Mankel, I.-A. Melzer-Pellmann, A.B. Meyer, G. Mittag, J. Mnich, A. Mussgiller, E. Ntomari, D. Pitzl, R. Placakyte, A. Raspereza, B. Roland, M.Ö. Sahin, P. Saxena, T. Schoerner-Sadenius, C. Seitz, S. Spannagel, N. Stefaniuk, K.D. Trippkewitz, G.P. Van Onsem, R. Walsh, C. Wissing

University of Hamburg, Hamburg, Germany
V. Blobel, M. Centis Vignali, A.R. Draeger, T. Dreyer, J. Erfle, E. Garutti, K. Goebel, D. Gonzalez, M. Görner, J. Haller, M. Hoffmann, R.S. Höing, A. Junkes, R. Klanner, R. Kogler, N. Kovalchuk, T. Lapsien, T. Lenz, I. Marchesini, D. Marconi, M. Meyer, M. Niedziela, D. Nowatschin, J. Ott, F. Pantaleo[13], T. Peiffer, A. Perieanu, N. Pietsch, J. Poehlsen, C. Sander, C. Scharf, P. Schleper, E. Schlieckau, A. Schmidt, S. Schumann, J. Schwandt, H. Stadie, G. Steinbrück, F.M. Stober, H. Tholen, D. Troendle, E. Usai, L. Vanelderen, A. Vanhoefer, B. Vormwald

JHEP02(2017)096

Institut für Experimentelle Kernphysik, Karlsruhe, Germany
C. Barth, C. Baus, J. Berger, C. Böser, E. Butz, T. Chwalek, F. Colombo, W. De Boer, A. Descroix, A. Dierlamm, S. Fink, F. Frensch, R. Friese, M. Giffels, A. Gilbert, D. Haitz, F. Hartmann[13], S.M. Heindl, U. Husemann, I. Katkov[14], A. Kornmayer[13], P. Lobelle Pardo, B. Maier, H. Mildner, M.U. Mozer, T. Müller, Th. Müller, M. Plagge, G. Quast, K. Rabbertz, S. Röcker, F. Roscher, M. Schröder, G. Sieber, H.J. Simonis, R. Ulrich, J. Wagner-Kuhr, S. Wayand, M. Weber, T. Weiler, S. Williamson, C. Wöhrmann, R. Wolf

Institute of Nuclear and Particle Physics (INPP), NCSR Demokritos, Aghia Paraskevi, Greece
G. Anagnostou, G. Daskalakis, T. Geralis, V.A. Giakoumopoulou, A. Kyriakis, D. Loukas, A. Psallidas, I. Topsis-Giotis

National and Kapodistrian University of Athens, Athens, Greece
A. Agapitos, S. Kesisoglou, A. Panagiotou, N. Saoulidou, E. Tziaferi

University of Ioánnina, Ioánnina, Greece
I. Evangelou, G. Flouris, C. Foudas, P. Kokkas, N. Loukas, N. Manthos, I. Papadopoulos, E. Paradas, J. Strologas

MTA-ELTE Lendület CMS Particle and Nuclear Physics Group, Eötvös Loránd University
N. Filipovic

Wigner Research Centre for Physics, Budapest, Hungary
G. Bencze, C. Hajdu, P. Hidas, D. Horvath[18], F. Sikler, V. Veszpremi, G. Vesztergombi[19], A.J. Zsigmond

Institute of Nuclear Research ATOMKI, Debrecen, Hungary
N. Beni, S. Czellar, J. Karancsi[20], J. Molnar, Z. Szillasi

University of Debrecen, Debrecen, Hungary
M. Bartók[19], A. Makovec, P. Raics, Z.L. Trocsanyi, B. Ujvari

National Institute of Science Education and Research, Bhubaneswar, India
S. Choudhury[21], P. Mal, K. Mandal, A. Nayak, D.K. Sahoo, N. Sahoo, S.K. Swain

Panjab University, Chandigarh, India
S. Bansal, S.B. Beri, V. Bhatnagar, R. Chawla, N. Dhingra, R. Gupta, U.Bhawandeep, A.K. Kalsi, A. Kaur, M. Kaur, R. Kumar, A. Mehta, M. Mittal, J.B. Singh, G. Walia

University of Delhi, Delhi, India
Ashok Kumar, A. Bhardwaj, B.C. Choudhary, R.B. Garg, S. Keshri, A. Kumar, S. Malhotra, M. Naimuddin, N. Nishu, K. Ranjan, R. Sharma, V. Sharma

Saha Institute of Nuclear Physics, Kolkata, India
R. Bhattacharya, S. Bhattacharya, K. Chatterjee, S. Dey, S. Dutta, S. Ghosh, N. Majumdar, A. Modak, K. Mondal, S. Mukhopadhyay, S. Nandan, A. Purohit, A. Roy, D. Roy, S. Roy Chowdhury, S. Sarkar, M. Sharan

JHEP02(2017)096

Bhabha Atomic Research Centre, Mumbai, India

R. Chudasama, D. Dutta, V. Jha, V. Kumar, A.K. Mohanty[13], L.M. Pant, P. Shukla, A. Topkar

Tata Institute of Fundamental Research, Mumbai, India

T. Aziz, S. Banerjee, S. Bhowmik[22], R.M. Chatterjee, R.K. Dewanjee, S. Dugad, S. Ganguly, S. Ghosh, M. Guchait, A. Gurtu[23], Sa. Jain, G. Kole, S. Kumar, B. Mahakud, M. Maity[22], G. Majumder, K. Mazumdar, S. Mitra, G.B. Mohanty, B. Parida, T. Sarkar[22], N. Sur, B. Sutar, N. Wickramage[24]

Indian Institute of Science Education and Research (IISER), Pune, India

S. Chauhan, S. Dube, A. Kapoor, K. Kothekar, A. Rane, S. Sharma

Institute for Research in Fundamental Sciences (IPM), Tehran, Iran

H. Bakhshiansohi, H. Behnamian, S.M. Etesami[25], A. Fahim[26], M. Khakzad, M. Mohammadi Najafabadi, M. Naseri, S. Paktinat Mehdiabadi, F. Rezaei Hosseinabadi, B. Safarzadeh[27], M. Zeinali

University College Dublin, Dublin, Ireland

M. Felcini, M. Grunewald

INFN Sezione di Bari [a], Università di Bari [b], Politecnico di Bari [c], Bari, Italy

M. Abbrescia[a,b], C. Calabria[a,b], C. Caputo[a,b], A. Colaleo[a], D. Creanza[a,c], L. Cristella[a,b], N. De Filippis[a,c], M. De Palma[a,b], L. Fiore[a], G. Iaselli[a,c], G. Maggi[a,c], M. Maggi[a], G. Miniello[a,b], S. My[a,b], S. Nuzzo[a,b], A. Pompili[a,b], G. Pugliese[a,c], R. Radogna[a,b], A. Ranieri[a], G. Selvaggi[a,b], L. Silvestris[a,13], R. Venditti[a,b]

INFN Sezione di Bologna [a], Università di Bologna [b], Bologna, Italy

G. Abbiendi[a], C. Battilana[13], D. Bonacorsi[a,b], S. Braibant-Giacomelli[a,b], L. Brigliadori[a,b], R. Campanini[a,b], P. Capiluppi[a,b], A. Castro[a,b], F.R. Cavallo[a], S.S. Chhibra[a,b], G. Codispoti[a,b], M. Cuffiani[a,b], G.M. Dallavalle[a], F. Fabbri[a], A. Fanfani[a,b], D. Fasanella[a,b], P. Giacomelli[a], C. Grandi[a], L. Guiducci[a,b], S. Marcellini[a], G. Masetti[a], A. Montanari[a], F.L. Navarria[a,b], A. Perrotta[a], A.M. Rossi[a,b], T. Rovelli[a,b], G.P. Siroli[a,b], N. Tosi[a,b,13]

INFN Sezione di Catania [a], Università di Catania [b], Catania, Italy

G. Cappello[b], M. Chiorboli[a,b], S. Costa[a,b], A. Di Mattia[a], F. Giordano[a,b], R. Potenza[a,b], A. Tricomi[a,b], C. Tuve[a,b]

INFN Sezione di Firenze [a], Università di Firenze [b], Firenze, Italy

G. Barbagli[a], V. Ciulli[a,b], C. Civinini[a], R. D'Alessandro[a,b], E. Focardi[a,b], V. Gori[a,b], P. Lenzi[a,b], M. Meschini[a], S. Paoletti[a], G. Sguazzoni[a], L. Viliani[a,b,13]

INFN Laboratori Nazionali di Frascati, Frascati, Italy

L. Benussi, S. Bianco, F. Fabbri, D. Piccolo, F. Primavera[13]

INFN Sezione di Genova [a], Università di Genova [b], Genova, Italy

V. Calvelli[a,b], F. Ferro[a], M. Lo Vetere[a,b], M.R. Monge[a,b], E. Robutti[a], S. Tosi[a,b]

JHEP02(2017)096

INFN Sezione di Milano-Bicocca [a], Università di Milano-Bicocca [b], Milano, Italy

L. Brianza, M.E. Dinardo[a,b], S. Fiorendi[a,b], S. Gennai[a], R. Gerosa[a,b], A. Ghezzi[a,b], P. Govoni[a,b], S. Malvezzi[a], R.A. Manzoni[a,b,13], B. Marzocchi[a,b], D. Menasce[a], L. Moroni[a], M. Paganoni[a,b], D. Pedrini[a], S. Pigazzini, S. Ragazzi[a,b], N. Redaelli[a], T. Tabarelli de Fatis[a,b]

INFN Sezione di Napoli [a], Università di Napoli 'Federico II' [b], Napoli, Italy, Università della Basilicata [c], Potenza, Italy, Università G. Marconi [d], Roma, Italy

S. Buontempo[a], N. Cavallo[a,c], S. Di Guida[a,d,13], M. Esposito[a,b], F. Fabozzi[a,c], A.O.M. Iorio[a,b], G. Lanza[a], L. Lista[a], S. Meola[a,d,13], M. Merola[a], P. Paolucci[a,13], C. Sciacca[a,b], F. Thyssen

INFN Sezione di Padova [a], Università di Padova [b], Padova, Italy, Università di Trento [c], Trento, Italy

P. Azzi[a,13], N. Bacchetta[a], L. Benato[a,b], D. Bisello[a,b], A. Boletti[a,b], A. Branca[a,b], R. Carlin[a,b], P. Checchia[a], M. Dall'Osso[a,b,13], T. Dorigo[a], U. Dosselli[a], F. Gasparini[a,b], U. Gasparini[a,b], A. Gozzelino[a], K. Kanishchev[a,c], S. Lacaprara[a], M. Margoni[a,b], G. Maron[a,28], A.T. Meneguzzo[a,b], J. Pazzini[a,b,13], N. Pozzobon[a,b], P. Ronchese[a,b], F. Simonetto[a,b], E. Torassa[a], M. Tosi[a,b], S. Ventura[a], M. Zanetti, P. Zotto[a,b], A. Zucchetta[a,b,13]

INFN Sezione di Pavia [a], Università di Pavia [b], Pavia, Italy

A. Braghieri[a], A. Magnani[a,b], P. Montagna[a,b], S.P. Ratti[a,b], V. Re[a], C. Riccardi[a,b], P. Salvini[a], I. Vai[a,b], P. Vitulo[a,b]

INFN Sezione di Perugia [a], Università di Perugia [b], Perugia, Italy

L. Alunni Solestizi[a,b], G.M. Bilei[a], D. Ciangottini[a,b], L. Fanò[a,b], P. Lariccia[a,b], R. Leonardi[a,b], G. Mantovani[a,b], M. Menichelli[a], A. Saha[a], A. Santocchia[a,b]

INFN Sezione di Pisa [a], Università di Pisa [b], Scuola Normale Superiore di Pisa [c], Pisa, Italy

K. Androsov[a,29], P. Azzurri[a,13], G. Bagliesi[a], J. Bernardini[a], T. Boccali[a], R. Castaldi[a], M.A. Ciocci[a,29], R. Dell'Orso[a], S. Donato[a,c], G. Fedi, L. Foà[a,c†], A. Giassi[a], M.T. Grippo[a,29], F. Ligabue[a,c], T. Lomtadze[a], L. Martini[a,b], A. Messineo[a,b], F. Palla[a], A. Rizzi[a,b], A. Savoy-Navarro[a,30], P. Spagnolo[a], R. Tenchini[a], G. Tonelli[a,b], A. Venturi[a], P.G. Verdini[a]

INFN Sezione di Roma [a], Università di Roma [b], Roma, Italy

L. Barone[a,b], F. Cavallari[a], G. D'imperio[a,b,13], D. Del Re[a,b,13], M. Diemoz[a], S. Gelli[a,b], C. Jorda[a], E. Longo[a,b], F. Margaroli[a,b], P. Meridiani[a], G. Organtini[a,b], R. Paramatti[a], F. Preiato[a,b], S. Rahatlou[a,b], C. Rovelli[a], F. Santanastasio[a,b]

JHEP02(2017)096

INFN Sezione di Torino [a], Università di Torino [b], Torino, Italy, Università del Piemonte Orientale [c], Novara, Italy

N. Amapane[a,b], R. Arcidiacono[a,c,13], S. Argiro[a,b], M. Arneodo[a,c], N. Bartosik[a], R. Bellan[a,b], C. Biino[a], N. Cartiglia[a], M. Costa[a,b], R. Covarelli[a,b], A. Degano[a,b], N. Demaria[a], L. Finco[a,b], B. Kiani[a,b], C. Mariotti[a], S. Maselli[a], E. Migliore[a,b], V. Monaco[a,b], E. Monteil[a,b], M.M. Obertino[a,b], L. Pacher[a,b], N. Pastrone[a], M. Pelliccioni[a], G.L. Pinna Angioni[a,b], F. Ravera[a,b], A. Romero[a,b], M. Ruspa[a,c], R. Sacchi[a,b], V. Sola[a], A. Solano[a,b], A. Staiano[a]

INFN Sezione di Trieste [a], Università di Trieste [b], Trieste, Italy

S. Belforte[a], V. Candelise[a,b], M. Casarsa[a], F. Cossutti[a], G. Della Ricca[a,b], B. Gobbo[a], C. La Licata[a,b], A. Schizzi[a,b], A. Zanetti[a]

Kangwon National University, Chunchon, Korea

S.K. Nam

Kyungpook National University, Daegu, Korea

K. Butanov, D.H. Kim, G.N. Kim, M.S. Kim, D.J. Kong, S. Lee, S.W. Lee, Y.D. Oh, S.I. Pak, D.C. Son, H. Yusupov

Chonbuk National University, Jeonju, Korea

J.A. Brochero Cifuentes, H. Kim, T.J. Kim[31]

Chonnam National University, Institute for Universe and Elementary Particles, Kwangju, Korea

S. Song

Korea University, Seoul, Korea

S. Cho, S. Choi, Y. Go, D. Gyun, B. Hong, Y. Kim, B. Lee, K. Lee, K.S. Lee, S. Lee, J. Lim, S.K. Park, Y. Roh

Seoul National University, Seoul, Korea

H.D. Yoo

University of Seoul, Seoul, Korea

M. Choi, H. Kim, H. Kim, J.H. Kim, J.S.H. Lee, I.C. Park, G. Ryu, M.S. Ryu

Sungkyunkwan University, Suwon, Korea

Y. Choi, J. Goh, D. Kim, E. Kwon, J. Lee, I. Yu

Vilnius University, Vilnius, Lithuania

V. Dudenas, A. Juodagalvis, J. Vaitkus

National Centre for Particle Physics, Universiti Malaya, Kuala Lumpur, Malaysia

I. Ahmed, Z.A. Ibrahim, J.R. Komaragiri, M.A.B. Md Ali[32], F. Mohamad Idris[33], W.A.T. Wan Abdullah, M.N. Yusli, Z. Zolkapli

JHEP02(2017)096

Centro de Investigacion y de Estudios Avanzados del IPN, Mexico City, Mexico
E. Casimiro Linares, H. Castilla-Valdez, E. De La Cruz-Burelo, I. Heredia-De La Cruz[34], A. Hernandez-Almada, R. Lopez-Fernandez, J. Mejia Guisao, A. Sanchez-Hernandez

Universidad Iberoamericana, Mexico City, Mexico
S. Carrillo Moreno, F. Vazquez Valencia

Benemerita Universidad Autonoma de Puebla, Puebla, Mexico
I. Pedraza, H.A. Salazar Ibarguen, C. Uribe Estrada

Universidad Autónoma de San Luis Potosí, San Luis Potosí, Mexico
A. Morelos Pineda

University of Auckland, Auckland, New Zealand
D. Krofcheck

University of Canterbury, Christchurch, New Zealand
P.H. Butler

National Centre for Physics, Quaid-I-Azam University, Islamabad, Pakistan
A. Ahmad, M. Ahmad, Q. Hassan, H.R. Hoorani, W.A. Khan, T. Khurshid, M. Shoaib, M. Waqas

National Centre for Nuclear Research, Swierk, Poland
H. Bialkowska, M. Bluj, B. Boimska, T. Frueboes, M. Górski, M. Kazana, K. Nawrocki, K. Romanowska-Rybinska, M. Szleper, P. Traczyk, P. Zalewski

Institute of Experimental Physics, Faculty of Physics, University of Warsaw, Warsaw, Poland
G. Brona, K. Bunkowski, A. Byszuk[35], K. Doroba, A. Kalinowski, M. Konecki, J. Krolikowski, M. Misiura, M. Olszewski, M. Walczak

Laboratório de Instrumentação e Física Experimental de Partículas, Lisboa, Portugal
P. Bargassa, C. Beirão Da Cruz E Silva, A. Di Francesco, P. Faccioli, P.G. Ferreira Parracho, M. Gallinaro, J. Hollar, N. Leonardo, L. Lloret Iglesias, M.V. Nemallapudi, F. Nguyen, J. Rodrigues Antunes, J. Seixas, O. Toldaiev, D. Vadruccio, J. Varela, P. Vischia

Joint Institute for Nuclear Research, Dubna, Russia
S. Afanasiev, M. Gavrilenko, I. Golutvin, I. Gorbunov, A. Kamenev, V. Karjavin, A. Lanev, A. Malakhov, V. Matveev[36,37], P. Moisenz, V. Palichik, V. Perelygin, M. Savina, S. Shmatov, S. Shulha, N. Skatchkov, V. Smirnov, N. Voytishin, A. Zarubin

Petersburg Nuclear Physics Institute, Gatchina (St. Petersburg), Russia
V. Golovtsov, Y. Ivanov, V. Kim[38], E. Kuznetsova[39], P. Levchenko, V. Murzin, V. Oreshkin, I. Smirnov, V. Sulimov, L. Uvarov, S. Vavilov, A. Vorobyev

Institute for Nuclear Research, Moscow, Russia
Yu. Andreev, A. Dermenev, S. Gninenko, N. Golubev, A. Karneyeu, M. Kirsanov, N. Krasnikov, A. Pashenkov, D. Tlisov, A. Toropin

JHEP02(2017)096

Institute for Theoretical and Experimental Physics, Moscow, Russia

V. Epshteyn, V. Gavrilov, N. Lychkovskaya, V. Popov, I. Pozdnyakov, G. Safronov, A. Spiridonov, M. Toms, E. Vlasov, A. Zhokin

National Research Nuclear University 'Moscow Engineering Physics Institute' (MEPhI), Moscow, Russia

R. Chistov, M. Danilov, O. Markin, V. Rusinov, E. Tarkovskii

P.N. Lebedev Physical Institute, Moscow, Russia

V. Andreev, M. Azarkin[37], I. Dremin[37], M. Kirakosyan, A. Leonidov[37], G. Mesyats, S.V. Rusakov

Skobeltsyn Institute of Nuclear Physics, Lomonosov Moscow State University, Moscow, Russia

A. Baskakov, A. Belyaev, E. Boos, M. Dubinin[40], L. Dudko, A. Ershov, A. Gribushin, V. Klyukhin, O. Kodolova, I. Lokhtin, I. Miagkov, S. Obraztsov, S. Petrushanko, V. Savrin, A. Snigirev

State Research Center of Russian Federation, Institute for High Energy Physics, Protvino, Russia

I. Azhgirey, I. Bayshev, S. Bitioukov, V. Kachanov, A. Kalinin, D. Konstantinov, V. Krychkine, V. Petrov, R. Ryutin, A. Sobol, L. Tourtchanovitch, S. Troshin, N. Tyurin, A. Uzunian, A. Volkov

University of Belgrade, Faculty of Physics and Vinca Institute of Nuclear Sciences, Belgrade, Serbia

P. Adzic[41], P. Cirkovic, D. Devetak, J. Milosevic, V. Rekovic

Centro de Investigaciones Energéticas Medioambientales y Tecnológicas (CIEMAT), Madrid, Spain

J. Alcaraz Maestre, E. Calvo, M. Cerrada, M. Chamizo Llatas, N. Colino, B. De La Cruz, A. Delgado Peris, A. Escalante Del Valle, C. Fernandez Bedoya, J.P. Fernández Ramos, J. Flix, M.C. Fouz, P. Garcia-Abia, O. Gonzalez Lopez, S. Goy Lopez, J.M. Hernandez, M.I. Josa, E. Navarro De Martino, A. Pérez-Calero Yzquierdo, J. Puerta Pelayo, A. Quintario Olmeda, I. Redondo, L. Romero, M.S. Soares

Universidad Autónoma de Madrid, Madrid, Spain

J.F. de Trocóniz, M. Missiroli, D. Moran

Universidad de Oviedo, Oviedo, Spain

J. Cuevas, J. Fernandez Menendez, S. Folgueras, I. Gonzalez Caballero, E. Palencia Cortezon[13], J.M. Vizan Garcia

Instituto de Física de Cantabria (IFCA), CSIC-Universidad de Cantabria, Santander, Spain

I.J. Cabrillo, A. Calderon, J.R. Castiñeiras De Saa, E. Curras, P. De Castro Manzano, M. Fernandez, J. Garcia-Ferrero, G. Gomez, A. Lopez Virto, J. Marco, R. Marco,

JHEP02(2017)096

C. Martinez Rivero, F. Matorras, J. Piedra Gomez, T. Rodrigo, A.Y. Rodríguez-Marrero, A. Ruiz-Jimeno, L. Scodellaro, N. Trevisani, I. Vila, R. Vilar Cortabitarte

CERN, European Organization for Nuclear Research, Geneva, Switzerland

D. Abbaneo, E. Auffray, G. Auzinger, M. Bachtis, P. Baillon, A.H. Ball, D. Barney, A. Benaglia, L. Benhabib, G.M. Berruti, P. Bloch, A. Bocci, A. Bonato, C. Botta, H. Breuker, T. Camporesi, R. Castello, M. Cepeda, G. Cerminara, M. D'Alfonso, D. d'Enterria, A. Dabrowski, V. Daponte, A. David, M. De Gruttola, F. De Guio, A. De Roeck, E. Di Marco[42], M. Dobson, M. Dordevic, B. Dorney, T. du Pree, D. Duggan, M. Dünser, N. Dupont, A. Elliott-Peisert, G. Franzoni, J. Fulcher, W. Funk, D. Gigi, K. Gill, M. Girone, F. Glege, R. Guida, S. Gundacker, M. Guthoff, J. Hammer, P. Harris, J. Hegeman, V. Innocente, P. Janot, H. Kirschenmann, V. Knünz, M.J. Kortelainen, K. Kousouris, P. Lecoq, C. Lourenço, M.T. Lucchini, N. Magini, L. Malgeri, M. Mannelli, A. Martelli, L. Masetti, F. Meijers, S. Mersi, E. Meschi, F. Moortgat, S. Morovic, M. Mulders, H. Neugebauer, S. Orfanelli[43], L. Orsini, L. Pape, E. Perez, M. Peruzzi, A. Petrilli, G. Petrucciani, A. Pfeiffer, M. Pierini, D. Piparo, A. Racz, T. Reis, G. Rolandi[44], M. Rovere, M. Ruan, H. Sakulin, J.B. Sauvan, C. Schäfer, C. Schwick, M. Seidel, A. Sharma, P. Silva, M. Simon, P. Sphicas[45], J. Steggemann, M. Stoye, Y. Takahashi, D. Treille, A. Triossi, A. Tsirou, V. Veckalns[46], G.I. Veres[19], N. Wardle, H.K. Wöhri, A. Zagozdzinska[35], W.D. Zeuner

Paul Scherrer Institut, Villigen, Switzerland

W. Bertl, K. Deiters, W. Erdmann, R. Horisberger, Q. Ingram, H.C. Kaestli, D. Kotlinski, U. Langenegger, T. Rohe

Institute for Particle Physics, ETH Zurich, Zurich, Switzerland

F. Bachmair, L. Bäni, L. Bianchini, B. Casal, G. Dissertori, M. Dittmar, M. Donegà, P. Eller, C. Grab, C. Heidegger, D. Hits, J. Hoss, G. Kasieczka, P. Lecomte†, W. Lustermann, B. Mangano, M. Marionneau, P. Martinez Ruiz del Arbol, M. Masciovecchio, M.T. Meinhard, D. Meister, F. Micheli, P. Musella, F. Nessi-Tedaldi, F. Pandolfi, J. Pata, F. Pauss, G. Perrin, L. Perrozzi, M. Quittnat, M. Rossini, M. Schönenberger, A. Starodumov[47], M. Takahashi, V.R. Tavolaro, K. Theofilatos, R. Wallny

Universität Zürich, Zurich, Switzerland

T.K. Aarrestad, C. Amsler[48], L. Caminada, M.F. Canelli, V. Chiochia, A. De Cosa, C. Galloni, A. Hinzmann, T. Hreus, B. Kilminster, C. Lange, J. Ngadiuba, D. Pinna, G. Rauco, P. Robmann, D. Salerno, Y. Yang

National Central University, Chung-Li, Taiwan

K.H. Chen, T.H. Doan, Sh. Jain, R. Khurana, M. Konyushikhin, C.M. Kuo, W. Lin, Y.J. Lu, A. Pozdnyakov, S.S. Yu

National Taiwan University (NTU), Taipei, Taiwan

Arun Kumar, P. Chang, Y.H. Chang, Y.W. Chang, Y. Chao, K.F. Chen, P.H. Chen, C. Dietz, F. Fiori, U. Grundler, W.-S. Hou, Y. Hsiung, Y.F. Liu, R.-S. Lu, M. Miñano Moya, E. Petrakou, J.f. Tsai, Y.M. Tzeng

JHEP02(2017)096

Chulalongkorn University, Faculty of Science, Department of Physics, Bangkok, Thailand

B. Asavapibhop, K. Kovitanggoon, G. Singh, N. Srimanobhas, N. Suwonjandee

Cukurova University, Adana, Turkey

A. Adiguzel, M.N. Bakirci[49], S. Cerci[50], S. Damarseckin, Z.S. Demiroglu, C. Dozen, E. Eskut, S. Girgis, G. Gokbulut, Y. Guler, E. Gurpinar, I. Hos, E.E. Kangal[51], G. Onengut[52], K. Ozdemir[53], A. Polatoz, D. Sunar Cerci[50], H. Topakli[49], C. Zorbilmez

Middle East Technical University, Physics Department, Ankara, Turkey

B. Bilin, S. Bilmis, B. Isildak[54], G. Karapinar[55], M. Yalvac, M. Zeyrek

Bogazici University, Istanbul, Turkey

E. Gülmez, M. Kaya[56], O. Kaya[57], E.A. Yetkin[58], T. Yetkin[59]

Istanbul Technical University, Istanbul, Turkey

A. Cakir, K. Cankocak, S. Sen[60], F.I. Vardarlı

Institute for Scintillation Materials of National Academy of Science of Ukraine, Kharkov, Ukraine

B. Grynyov

National Scientific Center, Kharkov Institute of Physics and Technology, Kharkov, Ukraine

L. Levchuk, P. Sorokin

University of Bristol, Bristol, United Kingdom

R. Aggleton, F. Ball, L. Beck, J.J. Brooke, D. Burns, E. Clement, D. Cussans, H. Flacher, J. Goldstein, M. Grimes, G.P. Heath, H.F. Heath, J. Jacob, L. Kreczko, C. Lucas, Z. Meng, D.M. Newbold[61], S. Paramesvaran, A. Poll, T. Sakuma, S. Seif El Nasr-storey, S. Senkin, D. Smith, V.J. Smith

Rutherford Appleton Laboratory, Didcot, United Kingdom

K.W. Bell, A. Belyaev[62], C. Brew, R.M. Brown, L. Calligaris, D. Cieri, D.J.A. Cockerill, J.A. Coughlan, K. Harder, S. Harper, E. Olaiya, D. Petyt, C.H. Shepherd-Themistocleous, A. Thea, I.R. Tomalin, T. Williams, S.D. Worm

Imperial College, London, United Kingdom

M. Baber, R. Bainbridge, O. Buchmuller, A. Bundock, D. Burton, S. Casasso, M. Citron, D. Colling, L. Corpe, P. Dauncey, G. Davies, A. De Wit, M. Della Negra, P. Dunne, A. Elwood, D. Futyan, Y. Haddad, G. Hall, G. Iles, R. Lane, R. Lucas[61], L. Lyons, A.-M. Magnan, S. Malik, L. Mastrolorenzo, J. Nash, A. Nikitenko[47], J. Pela, B. Penning, M. Pesaresi, D.M. Raymond, A. Richards, A. Rose, C. Seez, A. Tapper, K. Uchida, M. Vazquez Acosta[63], T. Virdee[13], S.C. Zenz

Brunel University, Uxbridge, United Kingdom

J.E. Cole, P.R. Hobson, A. Khan, P. Kyberd, D. Leslie, I.D. Reid, P. Symonds, L. Teodorescu, M. Turner

JHEP02(2017)096

Baylor University, Waco, U.S.A.

A. Borzou, K. Call, J. Dittmann, K. Hatakeyama, H. Liu, N. Pastika

The University of Alabama, Tuscaloosa, U.S.A.

O. Charaf, S.I. Cooper, C. Henderson, P. Rumerio

Boston University, Boston, U.S.A.

D. Arcaro, A. Avetisyan, T. Bose, D. Gastler, D. Rankin, C. Richardson, J. Rohlf, L. Sulak, D. Zou

Brown University, Providence, U.S.A.

J. Alimena, G. Benelli, E. Berry, D. Cutts, A. Ferapontov, A. Garabedian, J. Hakala, U. Heintz, O. Jesus, E. Laird, G. Landsberg, Z. Mao, M. Narain, S. Piperov, S. Sagir, R. Syarif

University of California, Davis, Davis, U.S.A.

R. Breedon, G. Breto, M. Calderon De La Barca Sanchez, S. Chauhan, M. Chertok, J. Conway, R. Conway, P.T. Cox, R. Erbacher, G. Funk, M. Gardner, W. Ko, R. Lander, C. Mclean, M. Mulhearn, D. Pellett, J. Pilot, F. Ricci-Tam, S. Shalhout, J. Smith, M. Squires, D. Stolp, M. Tripathi, S. Wilbur, R. Yohay

University of California, Los Angeles, U.S.A.

R. Cousins, P. Everaerts, A. Florent, J. Hauser, M. Ignatenko, D. Saltzberg, E. Takasugi, V. Valuev, M. Weber

University of California, Riverside, Riverside, U.S.A.

K. Burt, R. Clare, J. Ellison, J.W. Gary, G. Hanson, J. Heilman, M. Ivova PANEVA, P. Jandir, E. Kennedy, F. Lacroix, O.R. Long, M. Malberti, M. Olmedo Negrete, A. Shrinivas, H. Wei, S. Wimpenny, B. R. Yates

University of California, San Diego, La Jolla, U.S.A.

J.G. Branson, G.B. Cerati, S. Cittolin, R.T. D'Agnolo, M. Derdzinski, A. Holzner, R. Kelley, D. Klein, J. Letts, I. Macneill, D. Olivito, S. Padhi, M. Pieri, M. Sani, V. Sharma, S. Simon, M. Tadel, A. Vartak, S. Wasserbaech[64], C. Welke, J. Wood, F. Würthwein, A. Yagil, G. Zevi Della Porta

University of California, Santa Barbara, Santa Barbara, U.S.A.

J. Bradmiller-Feld, C. Campagnari, A. Dishaw, V. Dutta, K. Flowers, M. Franco Sevilla, P. Geffert, C. George, F. Golf, L. Gouskos, J. Gran, J. Incandela, N. Mccoll, S.D. Mullin, J. Richman, D. Stuart, I. Suarez, C. West, J. Yoo

California Institute of Technology, Pasadena, U.S.A.

D. Anderson, A. Apresyan, J. Bendavid, A. Bornheim, J. Bunn, Y. Chen, J. Duarte, A. Mott, H.B. Newman, C. Pena, M. Spiropulu, J.R. Vlimant, S. Xie, R.Y. Zhu

Carnegie Mellon University, Pittsburgh, U.S.A.

M.B. Andrews, V. Azzolini, A. Calamba, B. Carlson, T. Ferguson, M. Paulini, J. Russ, M. Sun, H. Vogel, I. Vorobiev

JHEP02(2017)096

University of Colorado Boulder, Boulder, U.S.A.

J.P. Cumalat, W.T. Ford, A. Gaz, F. Jensen, A. Johnson, M. Krohn, T. Mulholland, U. Nauenberg, K. Stenson, S.R. Wagner

Cornell University, Ithaca, U.S.A.

J. Alexander, A. Chatterjee, J. Chaves, J. Chu, S. Dittmer, N. Eggert, N. Mirman, G. Nicolas Kaufman, J.R. Patterson, A. Rinkevicius, A. Ryd, L. Skinnari, L. Soffi, W. Sun, S.M. Tan, W.D. Teo, J. Thom, J. Thompson, J. Tucker, Y. Weng, P. Wittich

Fermi National Accelerator Laboratory, Batavia, U.S.A.

S. Abdullin, M. Albrow, G. Apollinari, S. Banerjee, L.A.T. Bauerdick, A. Beretvas, J. Berryhill, P.C. Bhat, G. Bolla, K. Burkett, J.N. Butler, H.W.K. Cheung, F. Chlebana, S. Cihangir, V.D. Elvira, I. Fisk, J. Freeman, E. Gottschalk, L. Gray, D. Green, S. Grünendahl, O. Gutsche, J. Hanlon, D. Hare, R.M. Harris, S. Hasegawa, J. Hirschauer, Z. Hu, B. Jayatilaka, S. Jindariani, M. Johnson, U. Joshi, B. Klima, B. Kreis, S. Lammel, J. Lewis, J. Linacre, D. Lincoln, R. Lipton, T. Liu, R. Lopes De Sá, J. Lykken, K. Maeshima, J.M. Marraffino, S. Maruyama, D. Mason, P. McBride, P. Merkel, S. Mrenna, S. Nahn, C. Newman-Holmes†, V. O'Dell, K. Pedro, O. Prokofyev, G. Rakness, E. Sexton-Kennedy, A. Soha, W.J. Spalding, L. Spiegel, S. Stoynev, N. Strobbe, L. Taylor, S. Tkaczyk, N.V. Tran, L. Uplegger, E.W. Vaandering, C. Vernieri, M. Verzocchi, R. Vidal, M. Wang, H.A. Weber, A. Whitbeck

University of Florida, Gainesville, U.S.A.

D. Acosta, P. Avery, P. Bortignon, D. Bourilkov, A. Brinkerhoff, A. Carnes, M. Carver, D. Curry, S. Das, R.D. Field, I.K. Furic, J. Konigsberg, A. Korytov, K. Kotov, P. Ma, K. Matchev, H. Mei, P. Milenovic[65], G. Mitselmakher, D. Rank, R. Rossin, L. Shchutska, M. Snowball, D. Sperka, N. Terentyev, L. Thomas, J. Wang, S. Wang, J. Yelton

Florida International University, Miami, U.S.A.

S. Linn, P. Markowitz, G. Martinez, J.L. Rodriguez

Florida State University, Tallahassee, U.S.A.

A. Ackert, J.R. Adams, T. Adams, A. Askew, S. Bein, J. Bochenek, B. Diamond, J. Haas, S. Hagopian, V. Hagopian, K.F. Johnson, A. Khatiwada, H. Prosper, M. Weinberg

Florida Institute of Technology, Melbourne, U.S.A.

M.M. Baarmand, V. Bhopatkar, S. Colafranceschi[66], M. Hohlmann, H. Kalakhety, D. Noonan, T. Roy, F. Yumiceva

University of Illinois at Chicago (UIC), Chicago, U.S.A.

M.R. Adams, L. Apanasevich, D. Berry, R.R. Betts, I. Bucinskaite, R. Cavanaugh, O. Evdokimov, L. Gauthier, C.E. Gerber, D.J. Hofman, P. Kurt, C. O'Brien, I.D. Sandoval Gonzalez, P. Turner, N. Varelas, Z. Wu, M. Zakaria, J. Zhang

The University of Iowa, Iowa City, U.S.A.

B. Bilki[67], W. Clarida, K. Dilsiz, S. Durgut, R.P. Gandrajula, M. Haytmyradov, V. Khristenko, J.-P. Merlo, H. Mermerkaya[68], A. Mestvirishvili, A. Moeller, J. Nachtman, H. Ogul, Y. Onel, F. Ozok[69], A. Penzo, C. Snyder, E. Tiras, J. Wetzel, K. Yi

JHEP02(2017)096

Johns Hopkins University, Baltimore, U.S.A.

I. Anderson, B.A. Barnett, B. Blumenfeld, A. Cocoros, N. Eminizer, D. Fehling, L. Feng, A.V. Gritsan, P. Maksimovic, M. Osherson, J. Roskes, U. Sarica, M. Swartz, M. Xiao, Y. Xin, C. You

The University of Kansas, Lawrence, U.S.A.

P. Baringer, A. Bean, C. Bruner, J. Castle, R.P. Kenny III, A. Kropivnitskaya, D. Majumder, M. Malek, W. Mcbrayer, M. Murray, S. Sanders, R. Stringer, Q. Wang

Kansas State University, Manhattan, U.S.A.

A. Ivanov, K. Kaadze, S. Khalil, M. Makouski, Y. Maravin, A. Mohammadi, L.K. Saini, N. Skhirtladze, S. Toda

Lawrence Livermore National Laboratory, Livermore, U.S.A.

D. Lange, F. Rebassoo, D. Wright

University of Maryland, College Park, U.S.A.

C. Anelli, A. Baden, O. Baron, A. Belloni, B. Calvert, S.C. Eno, C. Ferraioli, J.A. Gomez, N.J. Hadley, S. Jabeen, R.G. Kellogg, T. Kolberg, J. Kunkle, Y. Lu, A.C. Mignerey, Y.H. Shin, A. Skuja, M.B. Tonjes, S.C. Tonwar

Massachusetts Institute of Technology, Cambridge, U.S.A.

A. Apyan, R. Barbieri, A. Baty, R. Bi, K. Bierwagen, S. Brandt, W. Busza, I.A. Cali, Z. Demiragli, L. Di Matteo, G. Gomez Ceballos, M. Goncharov, D. Gulhan, D. Hsu, Y. Iiyama, G.M. Innocenti, M. Klute, D. Kovalskyi, K. Krajczar, Y.S. Lai, Y.-J. Lee, A. Levin, P.D. Luckey, A.C. Marini, C. Mcginn, C. Mironov, S. Narayanan, X. Niu, C. Paus, C. Roland, G. Roland, J. Salfeld-Nebgen, G.S.F. Stephans, K. Sumorok, K. Tatar, M. Varma, D. Velicanu, J. Veverka, J. Wang, T.W. Wang, B. Wyslouch, M. Yang, V. Zhukova

University of Minnesota, Minneapolis, U.S.A.

A.C. Benvenuti, B. Dahmes, A. Evans, A. Finkel, A. Gude, P. Hansen, S. Kalafut, S.C. Kao, K. Klapoetke, Y. Kubota, Z. Lesko, J. Mans, S. Nourbakhsh, N. Ruckstuhl, R. Rusack, N. Tambe, J. Turkewitz

University of Mississippi, Oxford, U.S.A.

J.G. Acosta, S. Oliveros

University of Nebraska-Lincoln, Lincoln, U.S.A.

E. Avdeeva, R. Bartek, K. Bloom, S. Bose, D.R. Claes, A. Dominguez, C. Fangmeier, R. Gonzalez Suarez, R. Kamalieddin, D. Knowlton, I. Kravchenko, F. Meier, J. Monroy, F. Ratnikov, J.E. Siado, G.R. Snow, B. Stieger

State University of New York at Buffalo, Buffalo, U.S.A.

M. Alyari, J. Dolen, J. George, A. Godshalk, C. Harrington, I. Iashvili, J. Kaisen, A. Kharchilava, A. Kumar, A. Parker, S. Rappoccio, B. Roozbahani

JHEP02(2017)096

Northeastern University, Boston, U.S.A.

G. Alverson, E. Barberis, D. Baumgartel, M. Chasco, A. Hortiangtham, A. Massironi, D.M. Morse, D. Nash, T. Orimoto, R. Teixeira De Lima, D. Trocino, R.-J. Wang, D. Wood, J. Zhang

Northwestern University, Evanston, U.S.A.

S. Bhattacharya, K.A. Hahn, A. Kubik, J.F. Low, N. Mucia, N. Odell, B. Pollack, M.H. Schmitt, K. Sung, M. Trovato, M. Velasco

University of Notre Dame, Notre Dame, U.S.A.

N. Dev, M. Hildreth, C. Jessop, D.J. Karmgard, N. Kellams, K. Lannon, N. Marinelli, F. Meng, C. Mueller, Y. Musienko[36], M. Planer, A. Reinsvold, R. Ruchti, N. Rupprecht, G. Smith, S. Taroni, N. Valls, M. Wayne, M. Wolf, A. Woodard

The Ohio State University, Columbus, U.S.A.

L. Antonelli, J. Brinson, B. Bylsma, L.S. Durkin, S. Flowers, A. Hart, C. Hill, R. Hughes, W. Ji, T.Y. Ling, B. Liu, W. Luo, D. Puigh, M. Rodenburg, B.L. Winer, H.W. Wulsin

Princeton University, Princeton, U.S.A.

O. Driga, P. Elmer, J. Hardenbrook, P. Hebda, S.A. Koay, P. Lujan, D. Marlow, T. Medvedeva, M. Mooney, J. Olsen, C. Palmer, P. Piroué, D. Stickland, C. Tully, A. Zuranski

University of Puerto Rico, Mayaguez, U.S.A.

S. Malik

Purdue University, West Lafayette, U.S.A.

A. Barker, V.E. Barnes, D. Benedetti, D. Bortoletto, L. Gutay, M.K. Jha, M. Jones, A.W. Jung, K. Jung, D.H. Miller, N. Neumeister, B.C. Radburn-Smith, X. Shi, I. Shipsey, D. Silvers, J. Sun, A. Svyatkovskiy, F. Wang, W. Xie, L. Xu

Purdue University Calumet, Hammond, U.S.A.

N. Parashar, J. Stupak

Rice University, Houston, U.S.A.

A. Adair, B. Akgun, Z. Chen, K.M. Ecklund, F.J.M. Geurts, M. Guilbaud, W. Li, B. Michlin, M. Northup, B.P. Padley, R. Redjimi, J. Roberts, J. Rorie, Z. Tu, J. Zabel

University of Rochester, Rochester, U.S.A.

B. Betchart, A. Bodek, P. de Barbaro, R. Demina, Y.t. Duh, Y. Eshaq, T. Ferbel, M. Galanti, A. Garcia-Bellido, J. Han, O. Hindrichs, A. Khukhunaishvili, K.H. Lo, P. Tan, M. Verzetti

Rutgers, The State University of New Jersey, Piscataway, U.S.A.

J.P. Chou, E. Contreras-Campana, Y. Gershtein, E. Halkiadakis, M. Heindl, D. Hidas, E. Hughes, S. Kaplan, R. Kunnawalkam Elayavalli, A. Lath, K. Nash, H. Saka, S. Salur, S. Schnetzer, D. Sheffield, S. Somalwar, R. Stone, S. Thomas, P. Thomassen, M. Walker

JHEP02(2017)096

University of Tennessee, Knoxville, U.S.A.

M. Foerster, J. Heideman, G. Riley, K. Rose, S. Spanier, K. Thapa

Texas A&M University, College Station, U.S.A.

O. Bouhali[70], A. Castaneda Hernandez[70], A. Celik, M. Dalchenko, M. De Mattia, A. Delgado, S. Dildick, R. Eusebi, J. Gilmore, T. Huang, T. Kamon[71], V. Krutelyov, R. Mueller, I. Osipenkov, Y. Pakhotin, R. Patel, A. Perloff, L. Perniè, D. Rathjens, A. Rose, A. Safonov, A. Tatarinov, K.A. Ulmer

Texas Tech University, Lubbock, U.S.A.

N. Akchurin, C. Cowden, J. Damgov, C. Dragoiu, P.R. Dudero, J. Faulkner, S. Kunori, K. Lamichhane, S.W. Lee, T. Libeiro, S. Undleeb, I. Volobouev, Z. Wang

Vanderbilt University, Nashville, U.S.A.

E. Appelt, A.G. Delannoy, S. Greene, A. Gurrola, R. Janjam, W. Johns, C. Maguire, Y. Mao, A. Melo, H. Ni, P. Sheldon, S. Tuo, J. Velkovska, Q. Xu

University of Virginia, Charlottesville, U.S.A.

M.W. Arenton, P. Barria, B. Cox, B. Francis, J. Goodell, R. Hirosky, A. Ledovskoy, H. Li, C. Neu, T. Sinthuprasith, X. Sun, Y. Wang, E. Wolfe, F. Xia

Wayne State University, Detroit, U.S.A.

C. Clarke, R. Harr, P.E. Karchin, C. Kottachchi Kankanamge Don, P. Lamichhane, J. Sturdy

University of Wisconsin - Madison, Madison, WI, U.S.A.

D.A. Belknap, D. Carlsmith, S. Dasu, L. Dodd, S. Duric, B. Gomber, M. Grothe, M. Herndon, A. Hervé, P. Klabbers, A. Lanaro, A. Levine, K. Long, R. Loveless, A. Mohapatra, I. Ojalvo, T. Perry, G.A. Pierro, G. Polese, T. Ruggles, T. Sarangi, A. Savin, A. Sharma, N. Smith, W.H. Smith, D. Taylor, P. Verwilligen, N. Woods

†: Deceased
1: Also at Vienna University of Technology, Vienna, Austria
2: Also at State Key Laboratory of Nuclear Physics and Technology, Peking University, Beijing, China
3: Also at Institut Pluridisciplinaire Hubert Curien, Université de Strasbourg, Université de Haute Alsace Mulhouse, CNRS/IN2P3, Strasbourg, France
4: Also at Universidade Estadual de Campinas, Campinas, Brazil
5: Also at Centre National de la Recherche Scientifique (CNRS) - IN2P3, Paris, France
6: Also at Université Libre de Bruxelles, Bruxelles, Belgium
7: Also at Laboratoire Leprince-Ringuet, Ecole Polytechnique, IN2P3-CNRS, Palaiseau, France
8: Also at Joint Institute for Nuclear Research, Dubna, Russia
9: Now at British University in Egypt, Cairo, Egypt
10: Also at Zewail City of Science and Technology, Zewail, Egypt
11: Now at Ain Shams University, Cairo, Egypt
12: Also at Université de Haute Alsace, Mulhouse, France
13: Also at CERN, European Organization for Nuclear Research, Geneva, Switzerland

JHEP02(2017)096

14: Also at Skobeltsyn Institute of Nuclear Physics, Lomonosov Moscow State University, Moscow, Russia
15: Also at RWTH Aachen University, III. Physikalisches Institut A, Aachen, Germany
16: Also at University of Hamburg, Hamburg, Germany
17: Also at Brandenburg University of Technology, Cottbus, Germany
18: Also at Institute of Nuclear Research ATOMKI, Debrecen, Hungary
19: Also at MTA-ELTE Lendület CMS Particle and Nuclear Physics Group, Eötvös Loránd University, Budapest, Hungary
20: Also at University of Debrecen, Debrecen, Hungary
21: Also at Indian Institute of Science Education and Research, Bhopal, India
22: Also at University of Visva-Bharati, Santiniketan, India
23: Now at King Abdulaziz University, Jeddah, Saudi Arabia
24: Also at University of Ruhuna, Matara, Sri Lanka
25: Also at Isfahan University of Technology, Isfahan, Iran
26: Also at University of Tehran, Department of Engineering Science, Tehran, Iran
27: Also at Plasma Physics Research Center, Science and Research Branch, Islamic Azad University, Tehran, Iran
28: Also at Laboratori Nazionali di Legnaro dell'INFN, Legnaro, Italy
29: Also at Università degli Studi di Siena, Siena, Italy
30: Also at Purdue University, West Lafayette, U.S.A.
31: Now at Hanyang University, Seoul, Korea
32: Also at International Islamic University of Malaysia, Kuala Lumpur, Malaysia
33: Also at Malaysian Nuclear Agency, MOSTI, Kajang, Malaysia
34: Also at Consejo Nacional de Ciencia y Tecnología, Mexico city, Mexico
35: Also at Warsaw University of Technology, Institute of Electronic Systems, Warsaw, Poland
36: Also at Institute for Nuclear Research, Moscow, Russia
37: Now at National Research Nuclear University 'Moscow Engineering Physics Institute' (MEPhI), Moscow, Russia
38: Also at St. Petersburg State Polytechnical University, St. Petersburg, Russia
39: Also at University of Florida, Gainesville, U.S.A.
40: Also at California Institute of Technology, Pasadena, U.S.A.
41: Also at Faculty of Physics, University of Belgrade, Belgrade, Serbia
42: Also at INFN Sezione di Roma; Università di Roma, Roma, Italy
43: Also at National Technical University of Athens, Athens, Greece
44: Also at Scuola Normale e Sezione dell'INFN, Pisa, Italy
45: Also at National and Kapodistrian University of Athens, Athens, Greece
46: Also at Riga Technical University, Riga, Latvia
47: Also at Institute for Theoretical and Experimental Physics, Moscow, Russia
48: Also at Albert Einstein Center for Fundamental Physics, Bern, Switzerland
49: Also at Gaziosmanpasa University, Tokat, Turkey
50: Also at Adiyaman University, Adiyaman, Turkey
51: Also at Mersin University, Mersin, Turkey
52: Also at Cag University, Mersin, Turkey
53: Also at Piri Reis University, Istanbul, Turkey
54: Also at Ozyegin University, Istanbul, Turkey
55: Also at Izmir Institute of Technology, Izmir, Turkey
56: Also at Marmara University, Istanbul, Turkey
57: Also at Kafkas University, Kars, Turkey

JHEP02(2017)096

58: Also at Istanbul Bilgi University, Istanbul, Turkey
59: Also at Yildiz Technical University, Istanbul, Turkey
60: Also at Hacettepe University, Ankara, Turkey
61: Also at Rutherford Appleton Laboratory, Didcot, United Kingdom
62: Also at School of Physics and Astronomy, University of Southampton, Southampton, United Kingdom
63: Also at Instituto de Astrofísica de Canarias, La Laguna, Spain
64: Also at Utah Valley University, Orem, U.S.A.
65: Also at University of Belgrade, Faculty of Physics and Vinca Institute of Nuclear Sciences, Belgrade, Serbia
66: Also at Facoltà Ingegneria, Università di Roma, Roma, Italy
67: Also at Argonne National Laboratory, Argonne, U.S.A.
68: Also at Erzincan University, Erzincan, Turkey
69: Also at Mimar Sinan University, Istanbul, Istanbul, Turkey
70: Also at Texas A&M University at Qatar, Doha, Qatar
71: Also at Kyungpook National University, Daegu, Korea

JHEP02(2017)096